



ARL-TR-7277 • JUNE 2015



Development of Rolling Schedules for AZ31 Magnesium Alloy Sheets

by Laszlo Kecskes, Heidi Maupin, Vincent Hammond, Michael Eichhorst, Norman Herzig, and Lothar Meyer

Approved for public release; distribution is unlimited.

NOTICES

Disclaimers

The findings in this report are not to be construed as an official Department of the Army position unless so designated by other authorized documents.

Citation of manufacturer's or trade names does not constitute an official endorsement or approval of the use thereof.

Destroy this report when it is no longer needed. Do not return it to the originator.



Development of Rolling Schedules for AZ31 Magnesium Alloy Sheets

by Laszlo Kecskes, Heidi Maupin, and Vincent Hammond
Weapons and Materials Research Directorate, ARL

Michael Eichhorst, Norman Herzig, and Lothar Meyer
Nordmetall, GmbH, Neukirchen-Adorf, Germany

REPORT DOCUMENTATION PAGE				Form Approved OMB No. 0704-0188	
<p>Public reporting burden for this collection of information is estimated to average 1 hour per response, including the time for reviewing instructions, searching existing data sources, gathering and maintaining the data needed, and completing and reviewing the collection information. Send comments regarding this burden estimate or any other aspect of this collection of information, including suggestions for reducing the burden, to Department of Defense, Washington Headquarters Services, Directorate for Information Operations and Reports (0704-0188), 1215 Jefferson Davis Highway, Suite 1204, Arlington, VA 22202-4302. Respondents should be aware that notwithstanding any other provision of law, no person shall be subject to any penalty for failing to comply with a collection of information if it does not display a currently valid OMB control number.</p> <p>PLEASE DO NOT RETURN YOUR FORM TO THE ABOVE ADDRESS.</p>					
1. REPORT DATE (DD-MM-YYYY) June 2015		2. REPORT TYPE Final		3. DATES COVERED (From - To) May 2014	
4. TITLE AND SUBTITLE Development of Rolling Schedules for AZ31 Magnesium Alloy Sheets				5a. CONTRACT NUMBER	
				5b. GRANT NUMBER	
				5c. PROGRAM ELEMENT NUMBER	
6. AUTHOR(S) Laszlo Kecskes, Heidi Maupin, Vincent Hammond, Michael Eichhorst, Norman Herzig, and Lothar Meyer				5d. PROJECT NUMBER	
				5e. TASK NUMBER	
				5f. WORK UNIT NUMBER	
7. PERFORMING ORGANIZATION NAME(S) AND ADDRESS(ES) US Army Research Laboratory ATTN: RDRL-WMM-F Aberdeen Proving Ground, MD 21005-5069				8. PERFORMING ORGANIZATION REPORT NUMBER ARL-TR-7277	
9. SPONSORING/MONITORING AGENCY NAME(S) AND ADDRESS(ES)				10. SPONSOR/MONITOR'S ACRONYM(S)	
				11. SPONSOR/MONITOR'S REPORT NUMBER(S)	
12. DISTRIBUTION/AVAILABILITY STATEMENT Approved for public release; distribution is unlimited.					
13. SUPPLEMENTARY NOTES					
14. ABSTRACT <p>This report describes the effort to develop a low-temperature rolling procedure for as-received AZ31B, a magnesium (Mg) alloy that contains approximately 3% aluminum and 1% zinc. In particular, we investigated the ability to roll AZ31B to thicknesses of about 1.5 mm using conventional rolling temperatures. Next, attention was focused on reducing the rolling temperature as much as possible while still producing thin sheets (≤ 1.5-mm thickness) with an intent to retain a fine-grained microstructure. The ability to produce such thin sheets at as low a temperature as possible represented a significant challenge, which, if solved, could enable the development of ultrahigh-strength Mg alloy sheet for subsequent processing into high-strength components. Moreover, the results of this study would then could be used to develop further rolling schedules for other more complex Mg alloys via roll processing.</p>					
15. SUBJECT TERMS magnesium, AZ31, rolling, temperature, grain size					
16. SECURITY CLASSIFICATION OF:			17. LIMITATION OF ABSTRACT UU	18. NUMBER OF PAGES 60	19a. NAME OF RESPONSIBLE PERSON Laszlo Kecskes
a. REPORT Unclassified	b. ABSTRACT Unclassified	c. THIS PAGE Unclassified			19b. TELEPHONE NUMBER (Include area code) 410-306-0811

Standard Form 298 (Rev. 8/98)
Prescribed by ANSI Std. Z39.18

Contents

List of Figures	iv
List of Tables	vi
1. Introduction	1
2. Experimental Procedures	2
2.1 Materials	2
2.2 Hot Rolling	3
2.2 Sample Characterization: Microstructure and Tensile Properties	3
3. Rolling Experiments	5
3.1 High-Temperature Rolling	5
3.2 Influence of Rolling Direction on Lowest Rolling Temperature	7
4. Experimental Results	10
4.1 High-Temperature Rolling	10
4.1.1 Microstructure	10
4.1.2 Tensile Properties	23
4.2 Influence of Rolling Direction on Low-Temperature Rolling	26
4.2.1 Rolling Parallel to Original Rolling Direction	26
4.2.2 Rolling Transverse to Original Rolling Direction	39
5. Summary	47
6. Conclusions	48
7. References	50
List of Symbols, Abbreviations, and Acronyms	51
Distribution List	52

List of Figures

Fig. 1	Convection air furnace used for heat treatment studies	2
Fig. 2	Rolling mill (Hugo Sack GmbH).....	3
Fig. 3	Schematic of the tensile specimen	4
Fig. 4	Schematic of the universal testing machine.....	4
Fig. 5	Macrophotographs of the Mg plates for use in the first rolling experiments	5
Fig. 6	Orientation of the as-received plates relative to the original rolling direction	6
Fig. 7	Identification of rolling directions in this study with ORD in the as-supplied plate types: A-type plate = parallel to ORD, B-type plate = short transverse to ORD, and C-type plate = long transverse to ORD	8
Fig. 8	Rolling direction of the A-type plates (parallel to the ARL-rolling direction x)	9
Fig. 9	Rolling directions of the B- and C-type plates. For the B-type plate, the rolling direction is the short transverse direction, or crosswise to the x-axis and parallel to the z-axis of the ARL orientation. For C-type plate, the rolling direction is the long transverse direction, also crosswise to the x-axis, but, parallel to y-axis of the ARL orientation.	9
Fig. 10	Rolled sheets after rolling at high temperatures	10
Fig. 11	Location of microsections.....	11
Fig. 12	As-received material; outer zone	12
Fig. 13	As-received material; outer zone	12
Fig. 14	As-received material; outer zone	13
Fig. 15	As-received material; outer zone	13
Fig. 16	As-received material, outer zone; heat treated.....	13
Fig. 17	As-received material, outer zone; heat treated.....	14
Fig. 18	As-received material; inner zone	14
Fig. 19	As-received material; inner zone	14
Fig. 20	As-received material, inner zone; heat treated.....	15
Fig. 21	As-received material, inner zone; heat treated.....	15
Fig. 22	As-received material, inner zone; heat treated.....	15
Fig. 23	As-received material, inner zone; heat treated.....	16
Fig. 24	As-rolled microstructure; three rolling passes	17
Fig. 25	As-rolled microstructure; three rolling passes	17

Fig. 26	As-rolled microstructure; six rolling passes	17
Fig. 27	As-rolled microstructure; six rolling passes	18
Fig. 28	As-rolled microstructure; eight rolling passes	18
Fig. 29	Heat treated microstructure; eight rolling passes	19
Fig. 30	As-rolled microstructure; seven rolling passes	19
Fig. 31	Heat treated microstructure; seven rolling passes.....	19
Fig. 32	As-rolled microstructure; seven rolling passes	20
Fig. 33	Heat treated microstructure; seven rolling passes.....	20
Fig. 34	As-rolled microstructure, two final passes, $T = 425\text{ }^{\circ}\text{C}$, sheet 2.2	20
Fig. 35	Heat treated microstructure, two final passes, $T = 425\text{ }^{\circ}\text{C}$, sheet 2.1	21
Fig. 36	As-rolled microstructure, one final pass, $T = 425\text{ }^{\circ}\text{C}$, sheet 4.2	21
Fig. 37	Heat treated microstructure, one final pass, $T = 425\text{ }^{\circ}\text{C}$, sheet 4.1	21
Fig. 38	As-rolled microstructure after, one final pass, $T = 300\text{ }^{\circ}\text{C}$, sheet 6.2.....	22
Fig. 39	Heat treated microstructure, one final pass, $T = 300\text{ }^{\circ}\text{C}$, sheet 6.1	22
Fig. 40	Results of the tensile tests of sheets 4.2 after 7 passes in the as-rolled condition	23
Fig. 41	Results of the tensile tests of sheets 3.2 after 8 passes in the as-rolled condition	24
Fig. 42	Results of the tensile tests of sheet 4.1 after 7 passes in the as-annealed condition	25
Fig. 43	Results of the tensile tests of sheet 3.1 after 8 passes in the as-annealed condition	25
Fig. 44	Macrographs of sheets 1-A2, 2-A1, and 2-A2	28
Fig. 45	Macrographs of sheets 3-A1, 3-A2, 4-A1, 5-A1, 5-A2, 6-A1, and 6-A2	29
Fig. 46	Edge cracks of sheet 5-A2	30
Fig. 47	Shear failure of the rolled sheets.....	30
Fig. 48	Microstructure of the as-received material (A-type plates) in the longitudinal direction (x-direction, x-y-plane)	32
Fig. 49	Microstructure of the as-received material (A-type plates) in the transverse direction (z-direction, y-z-plane)	33
Fig. 50	Microstructure of the as-received material (A-type plates) in the longitudinal direction (y-direction, x-z-plane).....	34
Fig. 51	Bimodal microstructure of sheet 4-A1 after rolling to a thickness of 1.5 mm, longitudinal to rolling direction (x-y-plane)	35
Fig. 52	Microstructure of sheets 4-A1 after rolling to a thickness of 3.4 mm, longitudinal to rolling direction in 2 magnifications (x-y-plane)	36

Fig. 53	Microstructure of sheet 5-A1 after rolling to a thickness of 1.5 mm, longitudinal to rolling direction (x-y-plane)	37
Fig. 54	Microstructure of sheet 6-A2 after rolling to a thickness of 1.5 mm, longitudinal to rolling direction (x-y-plane)	38
Fig. 55	Microstructure of sheet 6-A2 after rolling to a thickness of 1.5 mm, transverse to rolling direction (x-y-plane)	39
Fig. 56	Rolled B-type sheets 1-B1, 1-B2, 2-B1, and 2-B2	40
Fig. 57	Rolled C-type sheets 1-C and 2-C	41
Fig. 58	Microstructure of the 1-B2 sheet after rolling to a thickness of 1.4 mm, longitudinal to rolling direction (x-z-plane)	43
Fig. 59	Microstructure of the 1-B2 sheet after rolling to a thickness of 1.4 mm, transverse to rolling direction (x-y-plane)	44
Fig. 60	Microstructure of sheet 2-C after rolling to a thickness of 1.4 mm, transverse to rolling direction (x-z-plane).....	45
Fig. 61	Microstructure of sheet 2-C after rolling to a thickness of 1.4 mm, transverse to rolling direction (x-z-plane).....	46

List of Tables

Table 1	Rolling passes in the initial study	6
Table 2	Results from rolled sheets	7
Table 3	Microstructure of the sheets	11
Table 4	Rolling passes for A-type plates	27
Table 5	Results of rolling passes and average chord length of rolled sheets (longitudinal direction)	35
Table 6	Rolling pass, sheet thickness, and furnace temperature for B- and C-type plates	40
Table 7	Roller temperature at the completion of each rolling pass for B- and C-type plates	42
Table 8	Rolling passes, sheet thicknesses in millimeter and average chord length of rolled sheets B and C (transverse direction)	47

1. Introduction

Over the past 5 years, the US Army Research Laboratory (ARL) has been actively pursuing the development of lightweight material systems for protective and structural applications, especially in ground vehicles. Magnesium (Mg), due to its low density (~25% that of steel and 67% that of aluminum [Al]), is often considered to be the lightest metallic material with an untapped potential for such applications. However, while some Mg alloys are currently found in military and commercial use, they are still not as widely used as Al and titanium alloys. One key factor for their limited use is their lower strength than the other alloys. In an effort to increase the strength of Mg alloys and thereby overcome this critical limitation, ARL has dedicated significant effort into producing alloys with an ultrafine-grained microstructure using equal channel angular extrusion (ECAE).¹ This effort has resulted in Mg alloys with submicrometer grain sizes and tensile strength well over 400 MPa. Moreover, the ability to produce alloys with a nearly uniform texture has resulted in reduced anisotropy and elongations over 10%, both of which are highly promising for the ongoing development of these alloys.

Although the availability of Mg alloys in sheet form would enable their use in a broad range of additional applications, wrought Mg is difficult to produce in thin sheets because of its inherently low ductility. As a result, Mg sheet is often produced at temperatures exceeding 300 °C. Although this temperature provides the alloy with sufficient ductility, the alloy tends to experience an appreciable amount of dynamic recrystallization and grain growth that will reduce the strength of the material. The amount of recrystallization and grain growth is expected to be more pronounced in the ECAE-processed alloys because of the large amount of strain energy imparted to the material to obtain the highly refined, final grain structure. Any loss of strength is undesirable, especially in the ultrahigh-strength alloys produced by the ECAE process at ARL.

In an effort to develop a lower-temperature rolling procedure that would minimize the strength loss described, ARL partnered with Nordmetall GmbH, a research company in Germany that specializes in the processing and characterization of advanced metallic alloys. In anticipation of rolling ultrafine-grained Mg alloy plates produced by ARL, the effort described in this report has focused on as-received AZ31B, an Mg alloy that contains approximately 3% Al and 1% zinc. In particular, this effort will first investigate the ability to roll AZ31B to thicknesses of about 1.5 mm using conventional rolling temperatures. Next, attention would focus on reducing the rolling temperature as much as possible while still producing thin sheets (≤ 1.5 -mm thickness) with the desired fine microstructure. The ability to

produce such thin sheets at as low a temperature as possible represents a significant challenge, which if solved could enable the development of ultrahigh-strength Mg alloy sheet for subsequent processing into high-strength components. Moreover, the results of this study could then be used to develop the rolling schedules for post-ECAE processed materials by means of roll processing.

2. Experimental Procedures

2.1 Materials

Large block samples of various dimensions were cut into 152.4- × 152.4- × 12.7-mm plates from a “master” rolled AZ31B Mg tooling plate held at ARL. Three sets of rolling plate samples were cut from the blocks so that rolling trials could be performed in each of the 3 orthogonal directions (rolling, long transverse, or through the thickness). These 3 sets of plates were supplied to Nordmetall. Upon receipt, the plates were given an annealing heat treatment at 440° C for 1 h in a convection air furnace (Fig. 1).

This temperature was deemed to be sufficiently high to remove any strain imparted to the as-received plates during fabrication. Optical microscopy was performed on the annealed and rolled sample plates to determine the size distribution and structural evolution of the grains and their orientation due to the different rolling parameters used in the various trials. Tensile properties of the rolled sheets were measured at room temperature using quasi-static tensile tests.



Fig. 1 Convection air furnace used for heat treatment studies

2.2 Hot Rolling

The rolling experiments were performed in conjunction with the Technical University Bergakademie Freiberg, a leading university in Germany for the production of Mg sheet materials. After preheating, the initially 12.5-mm-thick plates were rolled to a thickness equal to or less than 1.5 mm. The hot rolling was performed on a dual rolling mill (Hugo Sack Mills GmbH, Dusseldorf, Germany) (see Fig. 2). The diameter of the roller was about 360 mm, with a maximum rolling force of 2,400 kN. The rollers are driven by a 160-kW electric motor capable of producing 30 kNm of torque. The rollers were preheated to about 120 °C with electric blankets before the rolling experiments, and a lubricant was sprayed on the rollers before each rolling pass. The rolling speed was about 1 m/s, a common rolling speed for AZ31. The variations in rolling passes are described in the following sections.



Fig. 2 Rolling mill (Hugo Sack GmbH)

2.2 Sample Characterization: Microstructure and Tensile Properties

Representative specimens were taken from the transverse and longitudinal directions of the as-received and rolled plates. The specimens were mounted in an epoxy resin and prepared using conventional metallographic techniques. A final etching using diluted picric acid was used to better reveal the underlying grain

structure. The grain size was characterized by linear interceptions of grain boundaries.

Dogbone-shaped tensile test specimens with a gauge length of approximately 15 mm (Fig. 3) were machined from the as-received and processed plates. Room temperature tensile tests were performed at quasi-static strain rates (10^{-3} s^{-1}) using a universal testing machine (Zwick/Roell Materials Testing Machines, Ulm, Germany). The maximum force exerted by the testing machine is 100 kN, with a testing velocity between 0 and 500 mm/min. The experimental setup is shown schematically in Fig. 4. The testing machine consists of a stiff frame, 2 ball-bearing screw spindles, and a crosshead connected with the ball-bearing screw spindles. The forces were measured with a load cell with a maximum force of 5 kN. The elongation was measured with a fine-displacement extensometer.

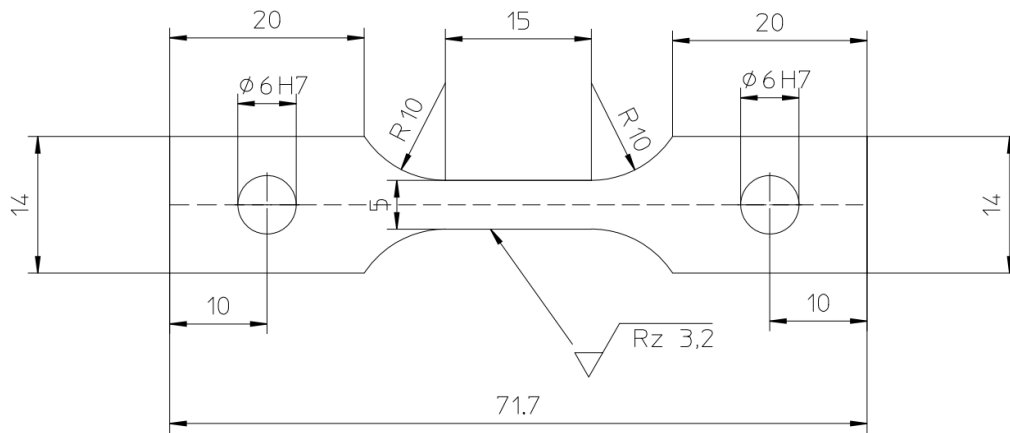


Fig. 3 Schematic of the tensile specimen

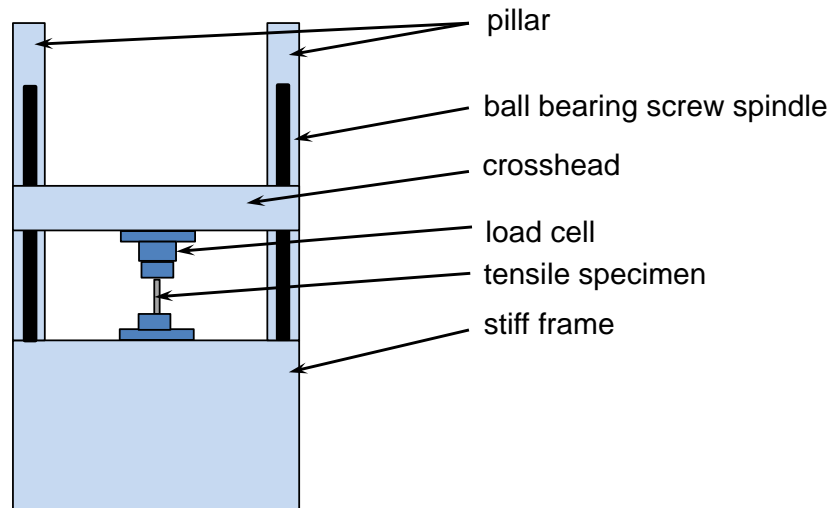


Fig. 4 Schematic of the universal testing machine

3. Rolling Experiments

The rolling experiments were conducted in 2 parts. In the first, the objective was to develop a rolling schedule to reduce the initial thickness of a plate to a final thickness of about 1.5 mm. In the second, the objective was to identify the lowest temperature whereby a plate could be rolled.

3.1 High-Temperature Rolling

Six plates with an approximate 152×152 -mm cross section and thickness of 12.5 mm were delivered for the first series of rolling experiments (Fig. 5). With the exception of the first plate, each plate was cut in the middle, rendering a rolling plate sample to be approximately 76 mm wide \times 152 mm long \times 12.5 mm thick. Cutting the plates in half effectively doubled the number of available samples from 6 to 12 for the planned rolling tests. The first plate was sectioned into 3 roughly equal pieces. Thus the cutting process produced 13 plates. The rolling direction and rolling plane for the supplied plates are shown in Fig. 6.

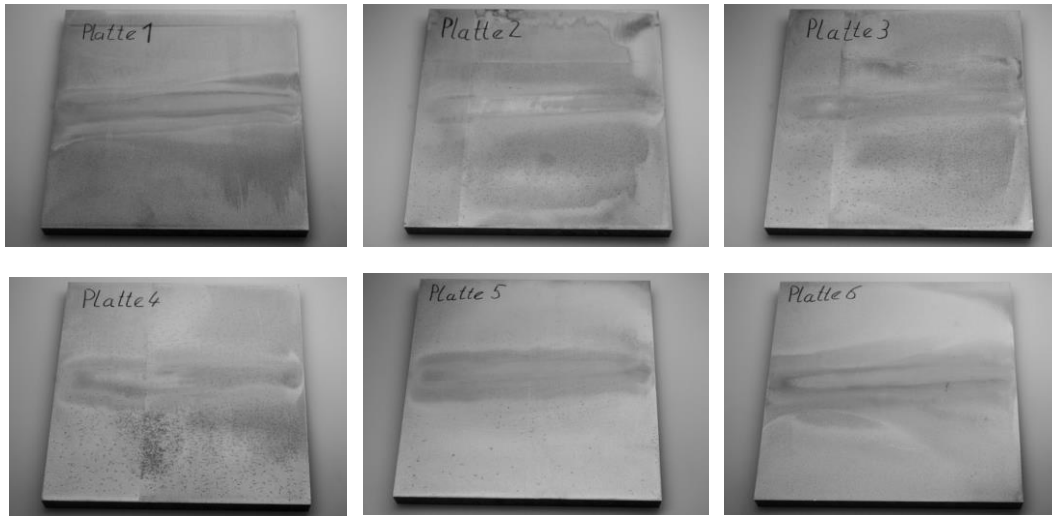


Fig. 5 Macrophotographs of the Mg plates for use in the first rolling experiments

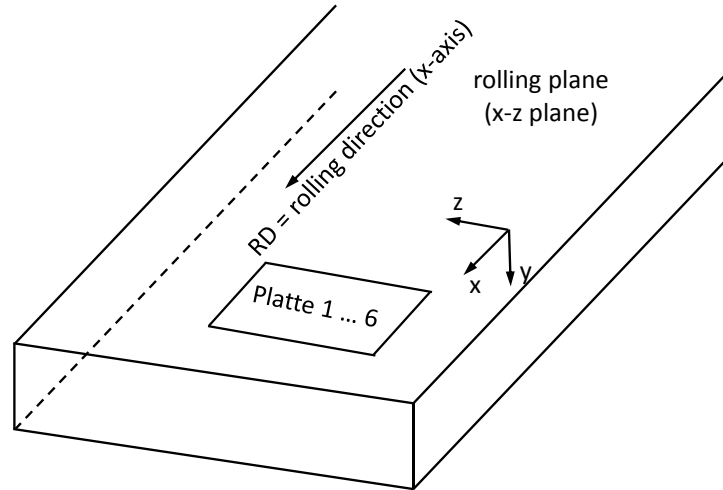


Fig. 6 Orientation of the as-received plates relative to the original rolling direction

Before starting the rolling experiments, the specimens were homogenized at 440 °C for 1 h in the convection air furnace. The sequence of steps of the rolling passes can be divided into 3 stages detailed in Table 1. After the end of the first and second stages, the sheets were annealed at 440 °C for 20 min. The results of the rolling experiments are detailed in Table 2.

Table 1 Rolling passes in the initial study

	Stage 1			Stage 2			Stage 3	
Rolling Pass	1	2	3	4	5	6	7	8
h_0 (mm)	12.5	10.0	7.8	6.1	4.5	3.3	2.4	(TS) 1.9
h_1 (mm)]	10.0	7.8	6.1	4.5	3.3	2.4	(TS)1.9 (OS) <1.5	(TS) <1.5

^aAnnealing at 440 °C for 20 min.

Note: h_0 = initial thickness; h_1 = final thickness

Table 2 Results from rolled sheets

No.	Temperature (°C)	Thickness (mm)	Number of Rolling Passes	Material Condition
1.1	425	6.1	3	As-rolled
1.2	425	2.4	6	As-rolled
1.3	425	<1.5	8 (final rolling with 2 passes)	As-rolled
2.1	425	<1.5	8 (final rolling with two passes)	Heat-treated ^a
2.2	425	<1.5	8 (final rolling with two passes)	As-rolled
3.1	425	<1.5	8 (final rolling with two passes)	Heat-treated ^a
3.2	425	<1.5	8 (final rolling with two passes)	As-rolled
4.1	425	<1.5	7 (final rolling with one pass)	Heat-treated ^a
4.2	425	<1.5	7 (final rolling with one pass)	As-rolled
5.1	425	<1.5	7 (final rolling with one pass)	Heat-treated ^a
5.2	425	<1.5	7 (final rolling with one pass)	As-rolled
6.1	300	<1.5	7 (final rolling with one pass)	Heat-treated ^a
6.2	300	<1.5	7 (final rolling with one pass)	As-rolled
	Metallographic investigation			

^aFinal heat treatment 330 ° C, 30 min

3.2 Influence of Rolling Direction on Lowest Rolling Temperature

The goal of the second part of this effort was to determine the lowest temperature at which quality Mg alloy sheet could be rolled. The rolling test matrix was designed so that a series of sheets were produced using different rolling conditions. In addition, the influence of the original rolling direction (ORD) in the as-supplied plates on rolling performance and sample quality was also of interest. To ensure consistent experimental conditions, the rolling direction of the as-received ARL tooling plate was always defined as the x-axis (see Fig. 7). Also shown in this figure are the orientations of the smaller plates cut from the as-supplied plates for use in the rolling experiments.

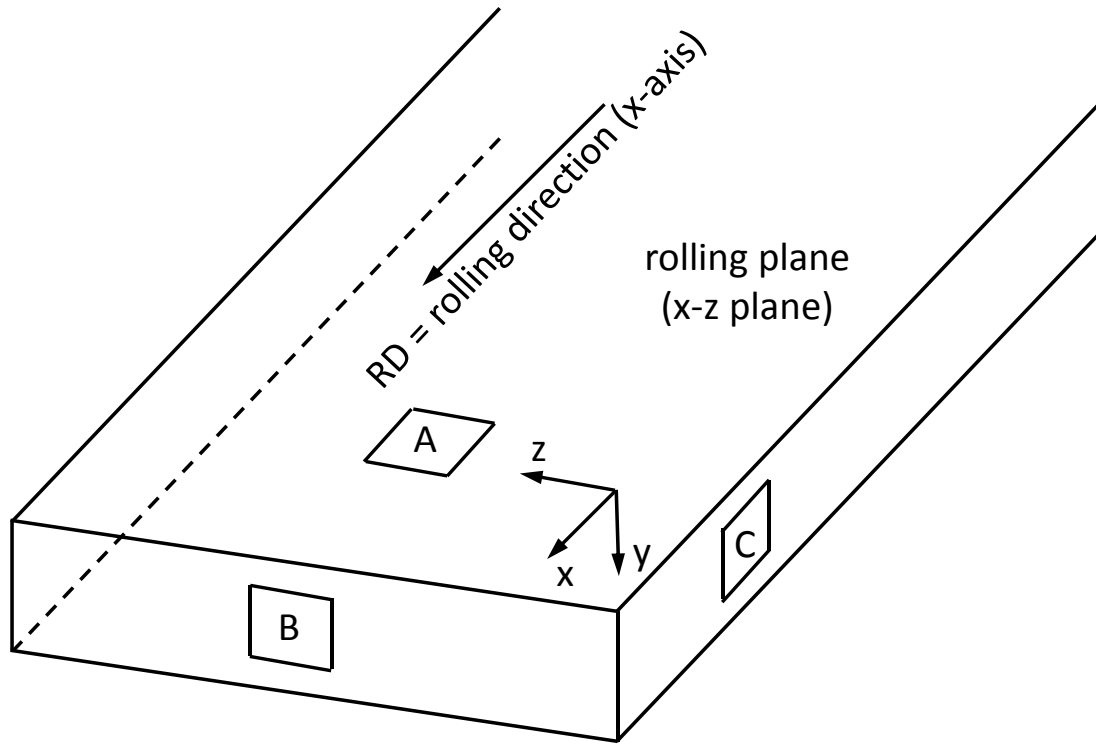


Fig. 7 Identification of rolling directions in this study with ORD in the as-supplied plate types: A-type plate = parallel to ORD, B-type plate = short transverse to ORD, and C-type plate = long transverse to ORD

As a first step for determining the lowest possible rolling temperature, 5 plates were rolled to produce sheets with a final thickness of about 1.5 mm without failure. For these plates, the rolling direction was oriented parallel to the rolling direction of the plates received from ARL (hereafter labeled as A-type plate). Each A- and B-type (short transverse to ORD) plate was cut along the middle, longitudinal to the rolling direction (see Figs. 8 and 9, respectively). Using the optimized temperature and rolling pass steps determined in the previous section, the plates labeled B and C (long transverse to ORD) were rolled from a thickness of about 12.5 mm down to ≤ 1.5 mm. The B-type plates were rolled in the z-direction while the C-type plates were rolled in the y-direction (see Fig. 9).

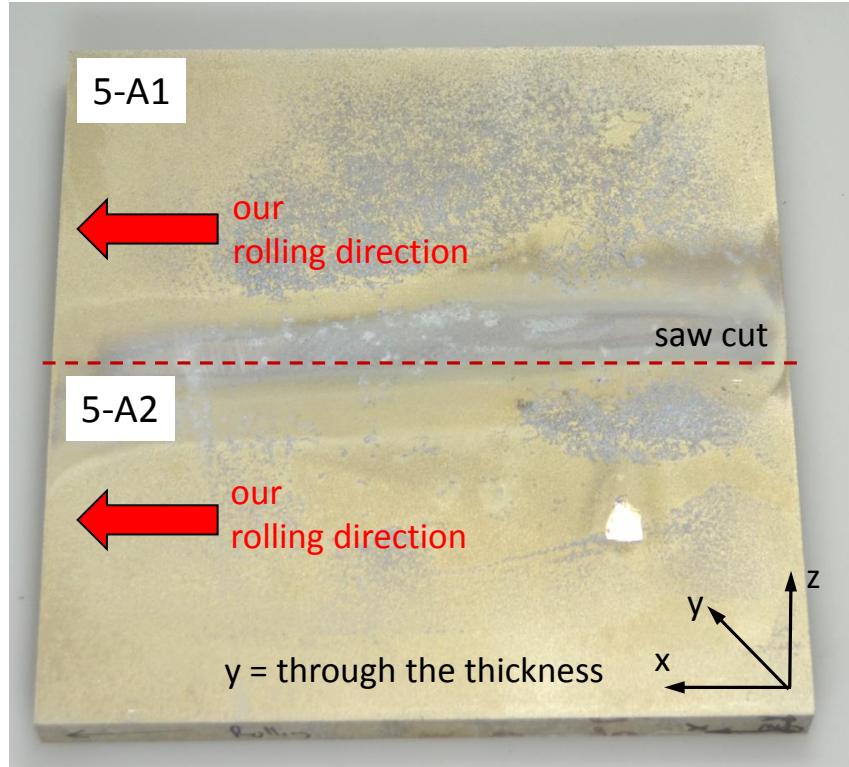


Fig. 8 Rolling direction of the A-type plates (parallel to the ARL-rolling direction x)

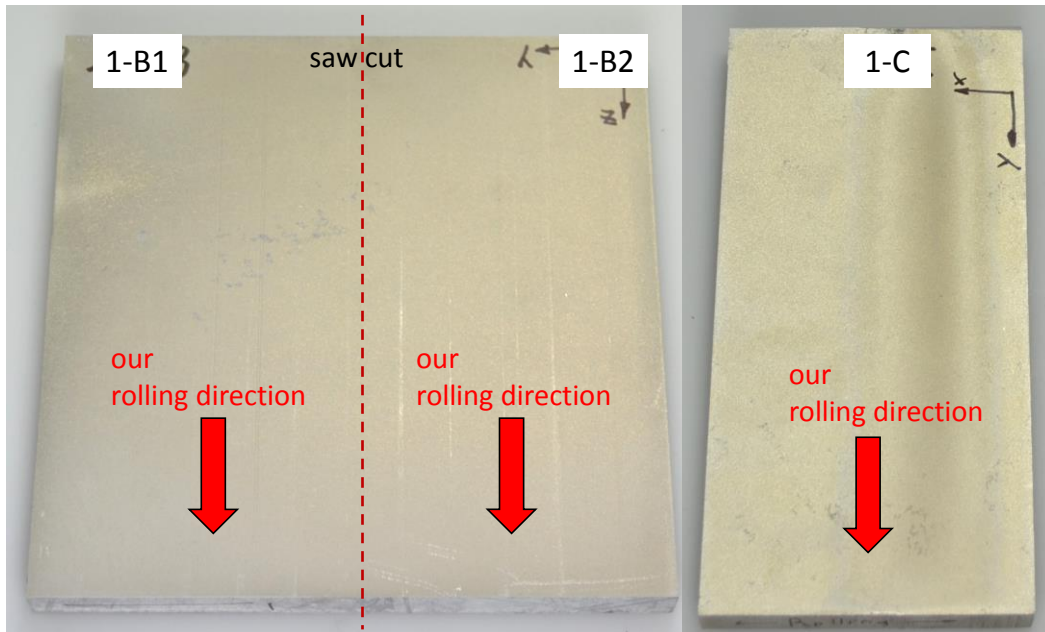


Fig. 9 Rolling directions of the B- and C-type plates. For the B-type plate, the rolling direction is the short transverse direction, or crosswise to the x-axis and parallel to the z-axis of the ARL orientation. For C-type plate, the rolling direction is the long transverse direction, also crosswise to the x-axis, but, parallel to y-axis of the ARL orientation.

4. Experimental Results

4.1 High-Temperature Rolling

4.1.1 Microstructure

Examples of rolled sheets are shown in Fig. 10. Sheets 1.1 and 1.2 were rolled to a thickness of about 6.1 and 2.4 mm, respectively. The surface quality of the sheets after rolling was very good, with no obvious cracks or failures observed in any sheets. The sheets have a maximum length of about 1.0–1.3 m.



Fig. 10 Rolled sheets after rolling at high temperatures

The results of the microstructural analysis and the material condition are listed in Table 3. The relative location of the microsections (outer and inner zone) are illustrated in Fig. 11. The microstructures (all oriented in the longitudinal direction) of all material conditions are shown in Figs. 12–33.

Table 3 Microstructure of the sheets

No.	Temperature (°C)	Thickness (mm)	Number of Rolling Passes	Material Condition	Grain Size Average Chord Length (μm)
1.1	425	6.1	3	As-rolled	13.4
1.2	425	2.4	6	As-rolled	5.8
2.1	425	<1.5	8 (final rolling with 2 passes)	Heat treated ^a	8.5
2.2	425	<1.5	8 (final rolling with 2 passes)	As-rolled	5.0
4.1	425	<1.5	7 (final rolling with 1 pass)	Heat treated ^a	5.7
4.2	425	<1.5	7 (final rolling with 1 pass)	As-rolled	6.7
6.1	300	<1.5	7 (final rolling with 1 pass)	Heat treated ^a	8.1
6.2	300	<1.5	7 (final rolling with one pass)	As-rolled	6.6

^aFinal heat treatment of 330 °C, 30 min

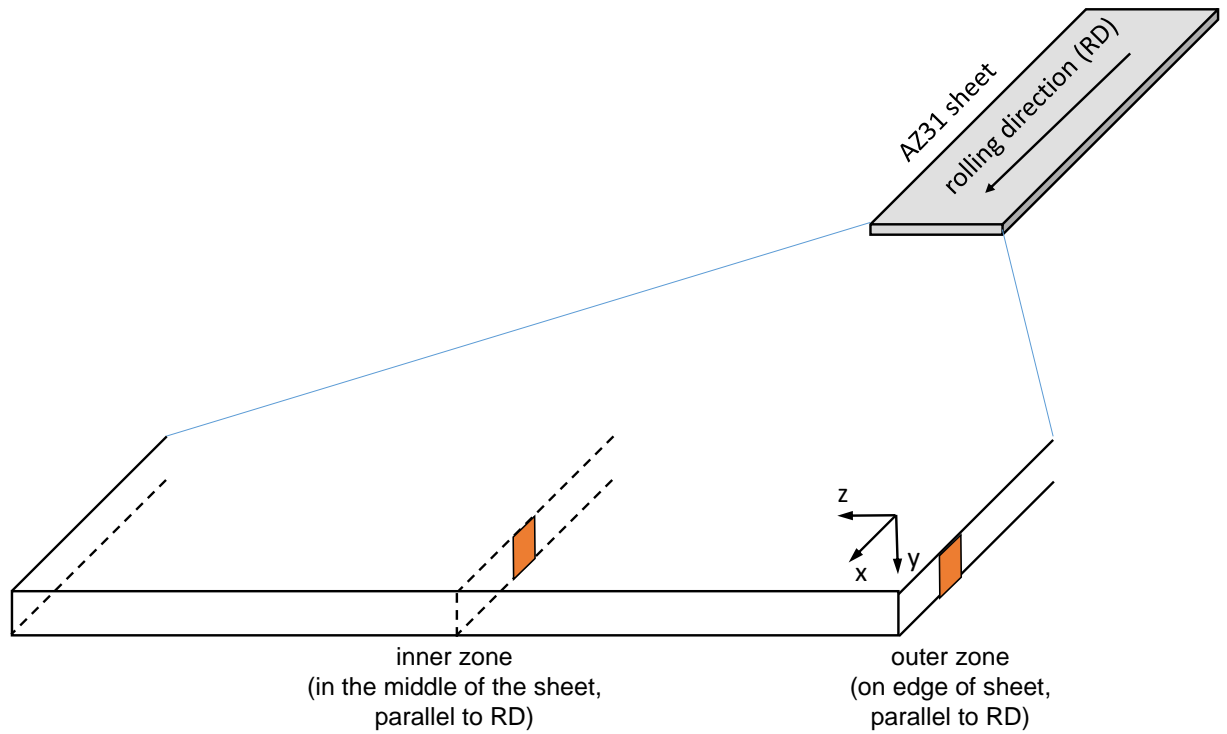


Fig. 11 Location of microsections

4.1.1.1 Microstructure of the As-Received Material, Inner and Outer Zone (Longitudinal Directional, x-y Plane)

The results of the microstructural analyses of the as-received tooling plate material, both inner and outer regions, (Figs. 12–15, 18, and 19) show a bimodal microstructure with grain sizes of about 50–300 μm . Without etching, in their as-polished states, the samples reveal little discernible detail, as can be seen in Figs. 12 and 13. However, after etching, there is much better detail, as Figs. 14 and 15 clearly illustrate the wide distribution in grain sizes. The black regions are precipitates that are known to occur in the AZ31 Mg alloy. The grain size remains nearly constant after annealing at 440 °C for 1 h (see Figs. 16, 17, and 20–23). In the latter higher magnification images, grains with dimensions of about 10–30 μm can be observed.

Polished
Magnification: 25×



Fig. 12 As-received material; outer zone

Polished
Magnification: 500×

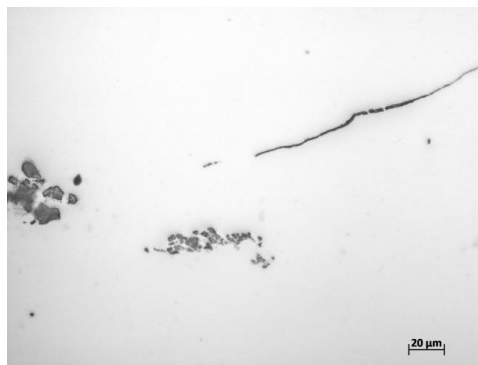


Fig. 13 As-received material; outer zone

Etched
Magnification: 25x

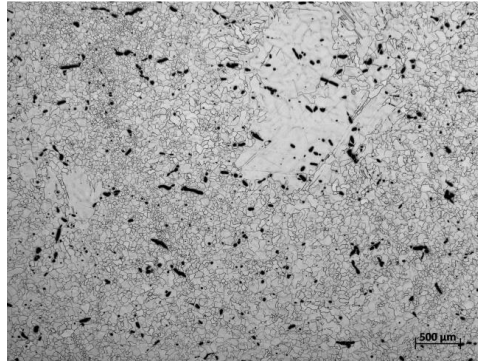


Fig. 14 As-received material; outer zone

Etched
Magnification: 200x

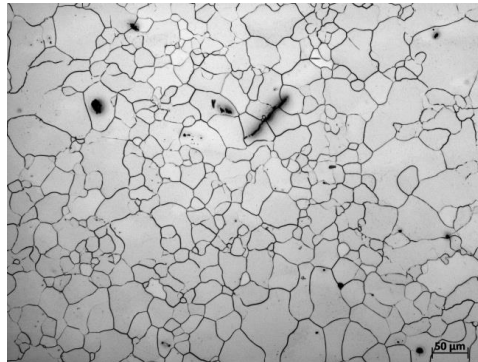


Fig. 15 As-received material; outer zone

Etched
Magnification: 25x

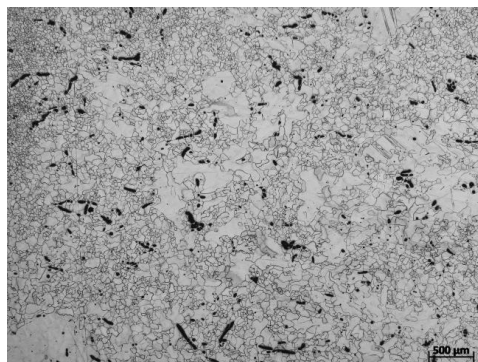


Fig. 16 As-received material, outer zone; heat treated

Etched
Magnification: 200×

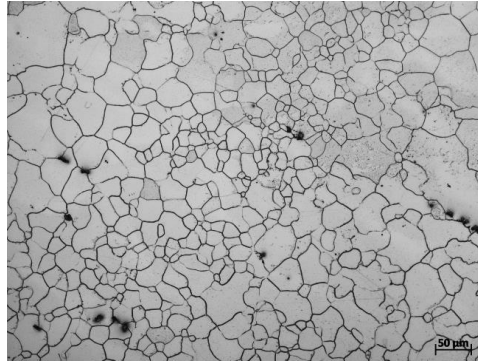


Fig. 17 As-received material, outer zone; heat treated

Etched
Magnification: 25×

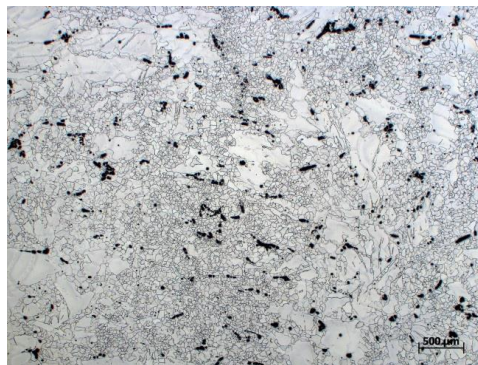


Fig. 18 As-received material; inner zone

Etched
Magnification: 200×

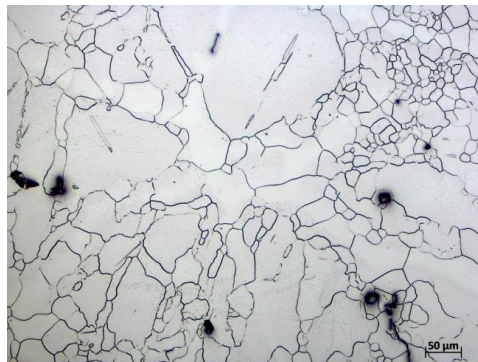


Fig. 19 As-received material; inner zone

Etched
Magnification: 25x

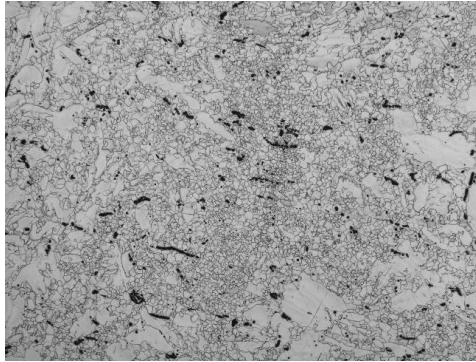


Fig. 20 As-received material, inner zone; heat treated

Etched
Magnification: 200x

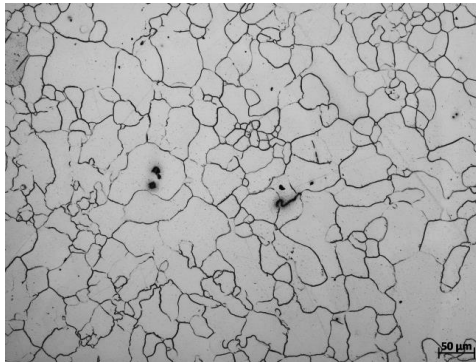


Fig. 21 As-received material, inner zone; heat treated

Etched
Magnification: 500x

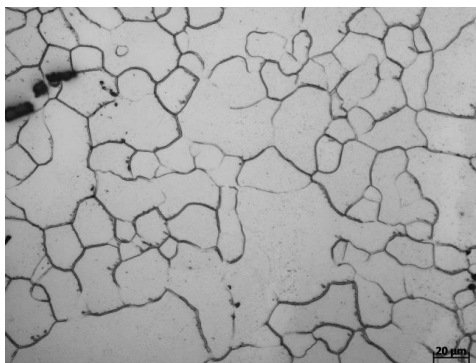


Fig. 22 As-received material, inner zone; heat treated

Etched
Magnification: 500×

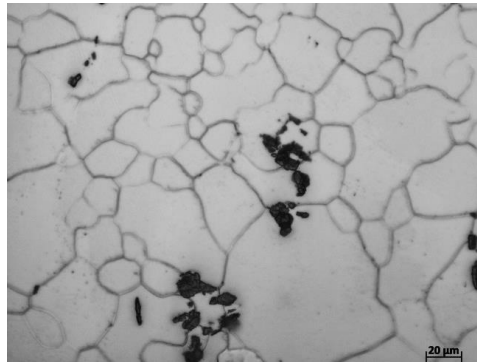


Fig. 23 As-received material, inner zone; heat treated

After rolling to a thickness of about 6.1 mm, the grain size was reduced significantly (see Figs. 24 and 25). More specifically, the clusters of larger grains that gave rise to the bimodal grain size distribution was broken up, resulting in a more uniform overall grain size distribution. The particles are oriented mainly parallel to the longitudinal direction; note the increasing alignment of the fine dark precipitates. With rolling to thicknesses of 2.4 mm (Figs. 26 and 27) and 1.5 mm (Figs. 28–39), respectively, further reduction in grain size can be observed. After final annealing, a slight increase in grain size was observed with grain sizes estimated between 4.2 and 5.1 μm before annealing and 5.5 to 8.8 μm after. The microstructure of the 1.5-mm sheets shows that the grains and precipitates are oriented in a chain-like manner, parallel to the rolling direction with a size of about 20–50 μm .

4.1.1.2 Microstructure after Stage 1 and Stage 2 Rolling (Longitudinal Direction, x-y plane)

Stage 1: After 3 rolling passes, thickness of the sheet is 6.1 mm.

Etched
Magnification: 25×

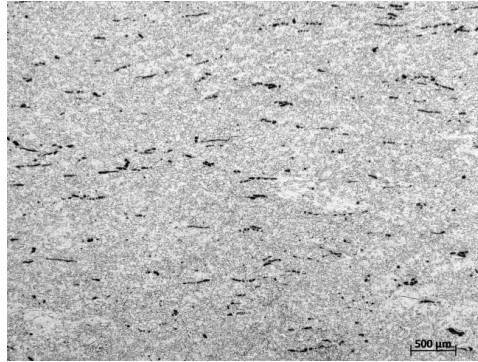


Fig. 24 As-rolled microstructure; three rolling passes

Etched
Magnification: 500×

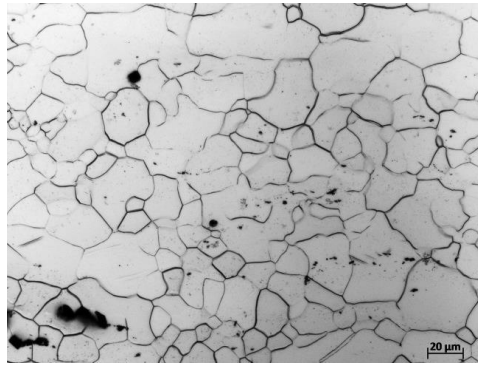


Fig. 25 As-rolled microstructure; three rolling passes

Stage 2: After 6 rolling passes, thickness of the sheet is 2.4 mm.

Etched
Magnification: 25×

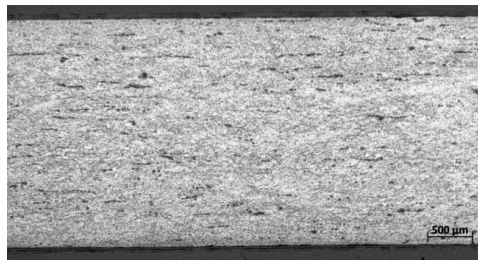


Fig. 26 As-rolled microstructure; six rolling passes

Etched
Magnification: 500x

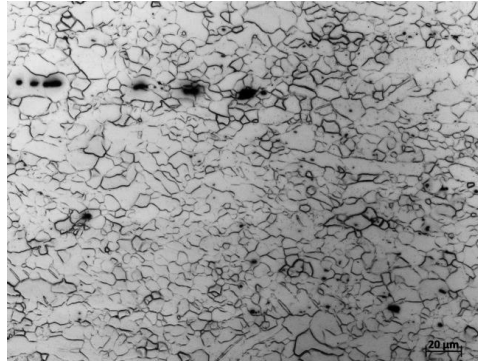


Fig. 27 As-rolled microstructure; six rolling passes

4.1.1.4 Microstructure after final rolling (500x magnification, longitudinal direction, x-y plane)

After eight or seven rolling passes, thickness of the sheet <1.5 m

Etched
Magnification 200x

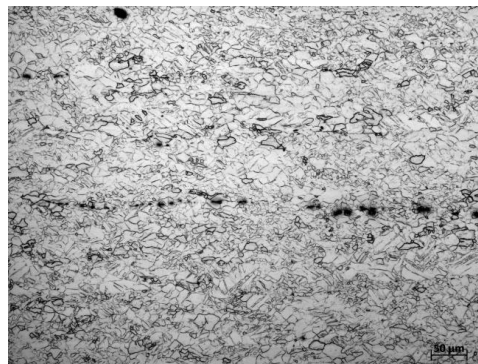


Fig. 28 As-rolled microstructure; eight rolling passes

Etched
Magnification 200x

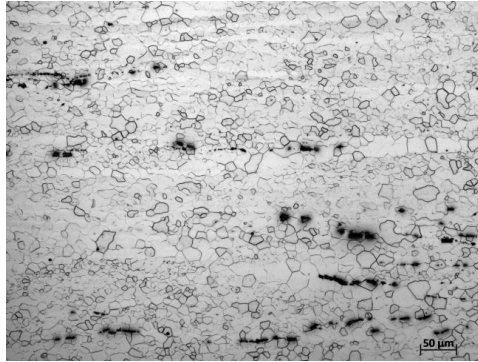


Fig. 29 Heat treated microstructure; eight rolling passes

Etched
Magnification 200x

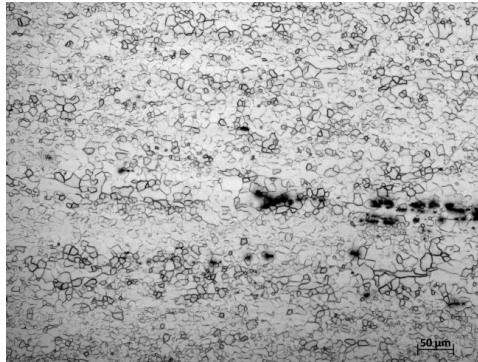


Fig. 30 As-rolled microstructure; seven rolling passes

Etched
Magnification 200x

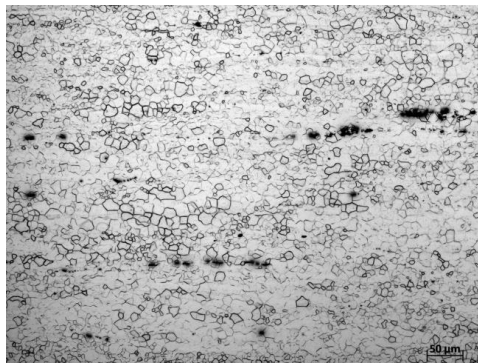


Fig. 31 Heat treated microstructure; seven rolling passes

Etched
Magnification 200×

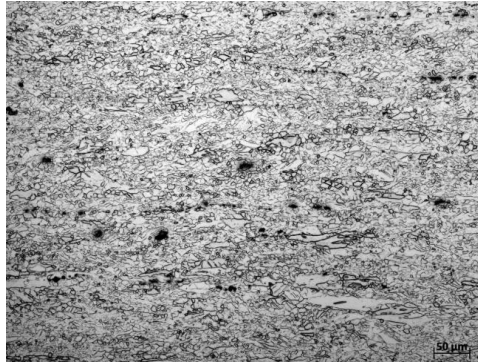


Fig. 32 As-rolled microstructure; seven rolling passes

Etched
Magnification 200×

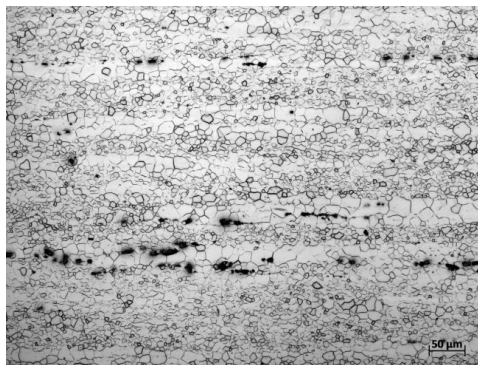


Fig. 33 Heat treated microstructure; seven rolling passes

Etched
Magnification: 500×

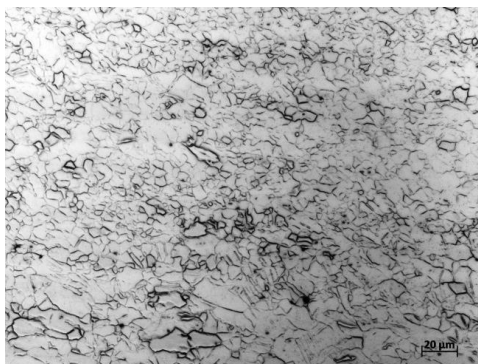


Fig. 34 As-rolled microstructure, two final passes, $T = 425\text{ }^{\circ}\text{C}$, sheet 2.2

Etched
Magnification: 500×

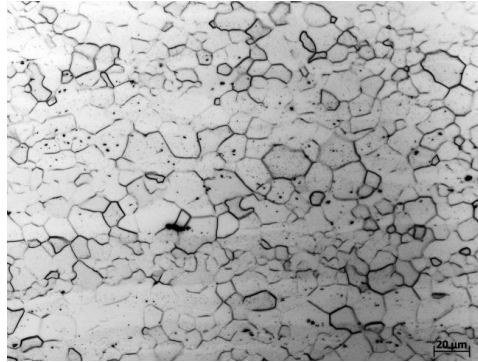


Fig. 35 Heat treated microstructure, two final passes, $T = 425\text{ }^{\circ}\text{C}$, sheet 2.1

Etched
Magnification: 500×

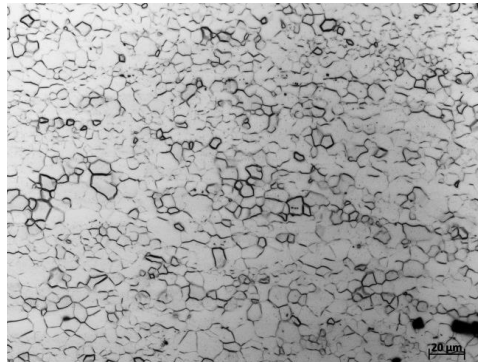


Fig. 36 As-rolled microstructure, one final pass, $T = 425\text{ }^{\circ}\text{C}$, sheet 4.2

Etched
Magnification: 500×

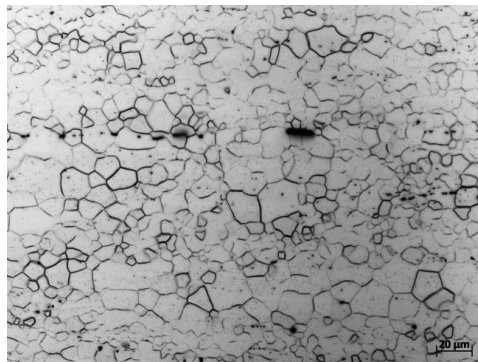


Fig. 37 Heat treated microstructure, one final pass, $T = 425\text{ }^{\circ}\text{C}$, sheet 4.1

Etched
Magnification: 500x

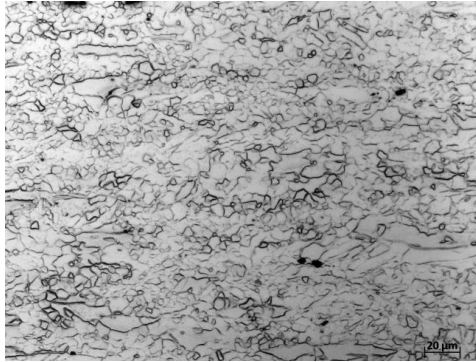


Fig. 38 As-rolled microstructure after, one final pass, $T = 300\text{ }^{\circ}\text{C}$, sheet 6.2

Etched
Magnification: 500x

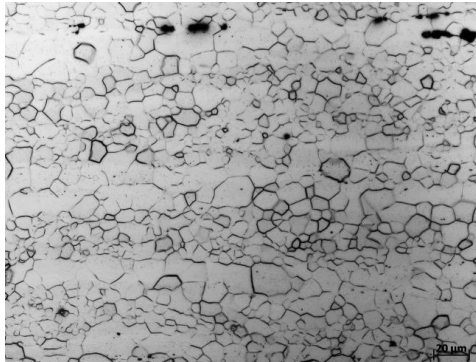


Fig. 39 Heat treated microstructure, one final pass, $T = 300\text{ }^{\circ}\text{C}$, sheet 6.1

4.1.2 Tensile Properties

Quasi-static tensile tests of the as-rolled and the post-rolled and annealed samples were conducted. The results of the tests of the as-rolled conditions are shown in Figs. 40 and 41. Nearly the same trend between all specimens for each orientation can be observed. The 1% yield stress ($\sigma_{1\%}$) in the longitudinal direction is slightly higher than that in the transverse direction. After 8 rolling passes, the ultimate tensile strength (UTS) in the longitudinal direction (about 280 MPa) is slightly higher than that after 7 rolling passes (about 270 MPa). All specimens failed at elongations of about 18%–23% engineering strain.

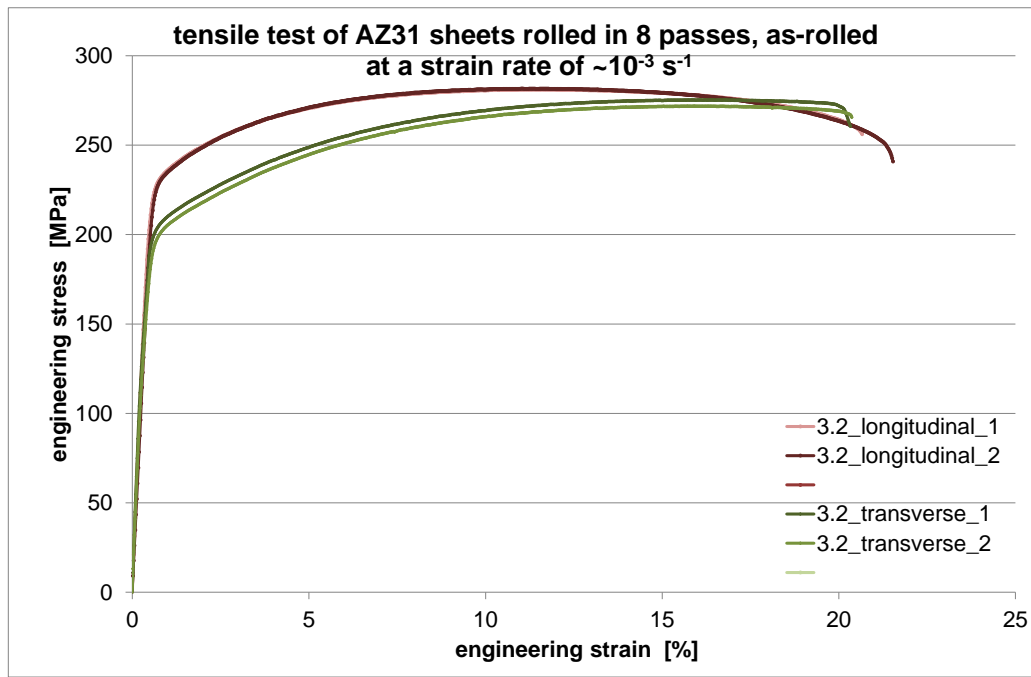


Fig. 40 Results of the tensile tests of sheets 4.2 after 7 passes in the as-rolled condition

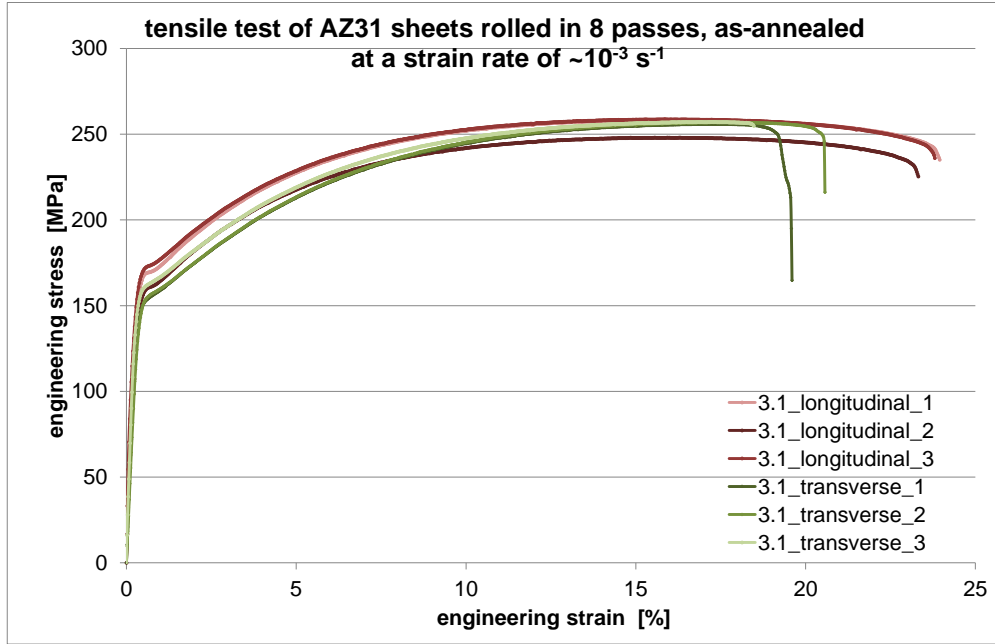


Fig. 41 Results of the tensile tests of sheets 3.2 after 8 passes in the as-rolled condition

The results of the tensile tests of the post-rolled and annealed sheets are shown in Figs. 42 and 43. Again, only slight deviations between specimens for each orientation can be observed. The strength ($\sigma_{1\%}$) in the longitudinal and transverse directions and the elongation to failure is nearly the same. It is believed that one specimen (with elongation to failure of about 14%) exhibited a defect before testing. The UTS (approximately 255 MPa) is essentially constant for the different as-annealed conditions.

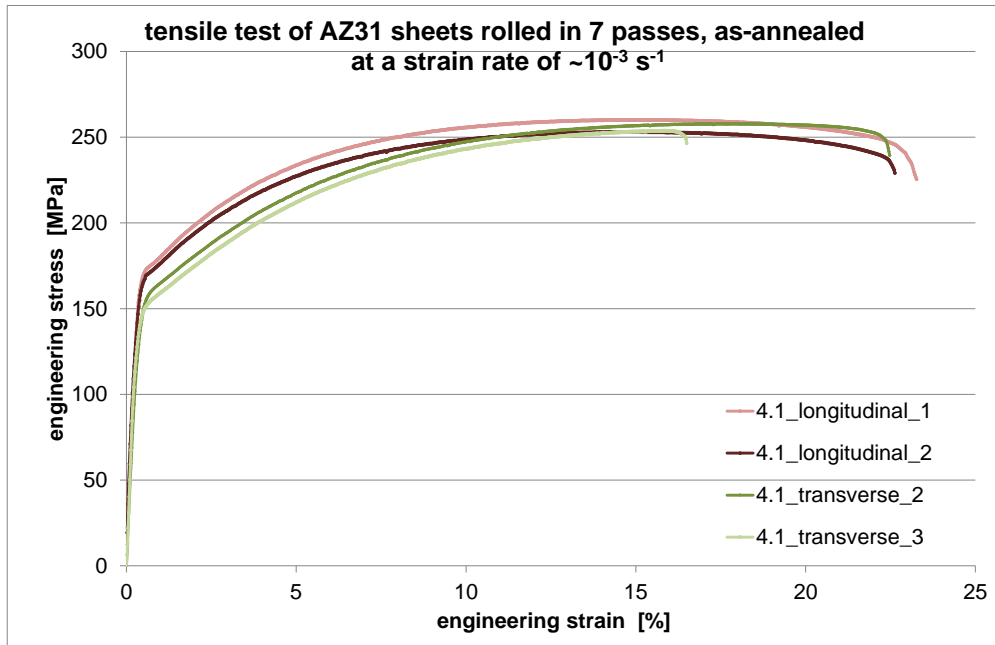


Fig. 42 Results of the tensile tests of sheet 4.1 after 7 passes in the as-annealed condition

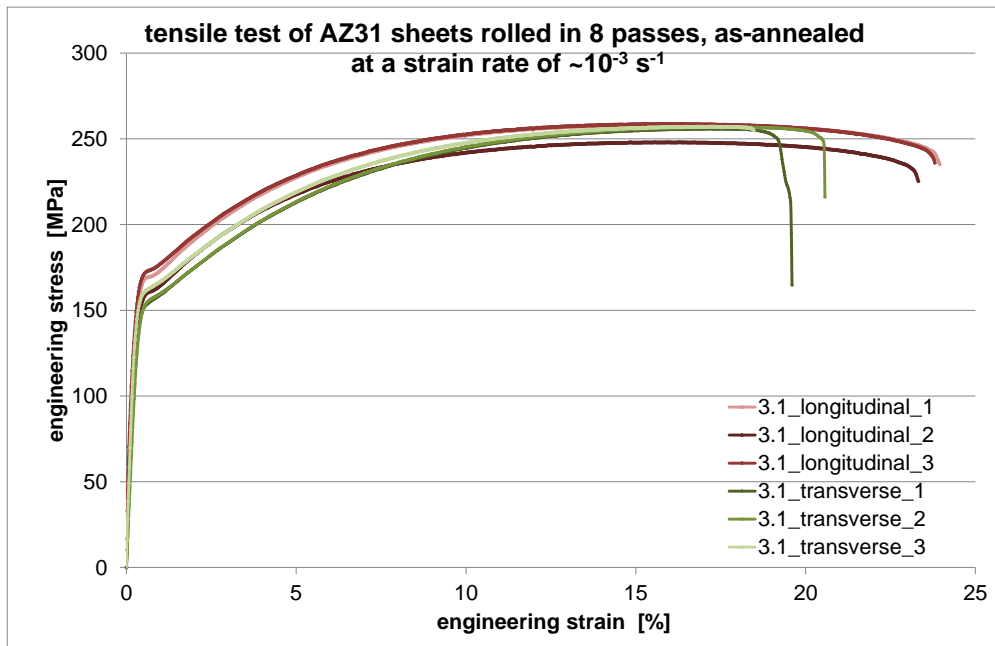


Fig. 43 Results of the tensile tests of sheet 3.1 after 8 passes in the as-annealed condition

Comparing the as-rolled and the as-annealed material conditions, a higher strength ($\sigma_{1\%}$) and UTS can be observed for the as-rolled material. In contrast, elongation at failure is nearly the same. This means a final annealing after rolling to enhance the ductility is not leading to a noticeable advantage.

4.2 Influence of Rolling Direction on Low-Temperature Rolling

4.2.1 Rolling Parallel to Original Rolling Direction

Six plates in the A orientation were sectioned from the master block supplied by ARL. As indicated earlier, these were cut in approximately equal halves, yielding 12 samples. Samples were identified by plate number, orientation, and either as 1 or 2 (for example 1-A1 or 1-A2). Of these, 10 samples were used in rolling experiments. Sample 1-A1 was used for metallographic evaluation of the initial material. Sample 4-A2 was used to measure the plate temperature during the prerolling heat treatment in the convection air furnace. In Table 44, the rolling passes and furnace temperatures for all A plates (rolling direction longitudinal to rolling direction of ARL) are listed. The maximum sheet length is about 1.0–1.1 m. Samples marked “failed” experienced a complete failure by shear across the width of the plate. As such, these plates were no longer suitable for further rolling passes.

In anticipation of rapid sample failure at too low of a rolling temperature, the first rolling experiments started with a furnace temperature of about 200 °C (plates 1-A2, 2-A1, and 2-A2). As our first test, plate 2-A2 was rolled to a thickness of about 3.3 mm at a temperature of about 200 °C; however, it failed after 6 rolling passes. Therefore, the furnace temperature was increased to 250 °C. By increasing the furnace temperature after the first or the second pass (see plates 1-A2 and 2-A1) 10–11 rolling passes were possible. However, despite this approach, plate 1-A2 failed after 11 rolling passes. Cracks on the edges were observed for plate 2-A1 (see Fig. 44).

Table 4 Rolling passes for A-type plates^a

Rolling Pass	Plate Number (thickness in mm)									
	1-A2	2-A1	2-A2	3-A1	3-A2	4-A1	5-A1	5-A2	6-A1	6-A2
1	10.0	10.0	10.0	10.0	10.0	10.0	10.6	10.6	10.6	10.6
2	8.0	8.2	8.2	8.2	8.0	8.0	9.0	9.0	9.0	9.0
3	6.4	6.4	6.4	6.4	6.4	6.7	7.7	7.7	6.9	6.8
4	5.3	5.3	5.1	5.1	5.2	6.1	6.5	6.2	6.2	6.2
5	4.9	4.7	4.1	4.1	4.7	5.4	5.7	5.4	5.7	5.7
6	4.4	4.0	3.3	3.2	4.0	4.7	4.7	4.7	4.7	4.7
7	3.9	3.5	3.4	4.0	4.0	4.0	4.0	4.0
8	3.4	2.9	2.9	3.4	3.4	3.4	3.4	3.4
9	2.9	2.5	2.5	2.9	2.9	2.9	2.9	2.9
10	2.5	2.2	2.2	2.1	2.1	2.1	2.1	2.2
11	2.1	1.5	1.5	1.5	1.5	1.5
...	Failed	Cracks on edge	Failed	Failed	Cracks on edge	Cracks on edge	Cracks on edge	Cracks on edge	Failed	Cracks on edge
Furnace Temperature [°C]	...	200								
	...	250								
	...	275								

^aIntermediate annealing for 15 min at the same furnace temperature as the next rolling pass was performed.

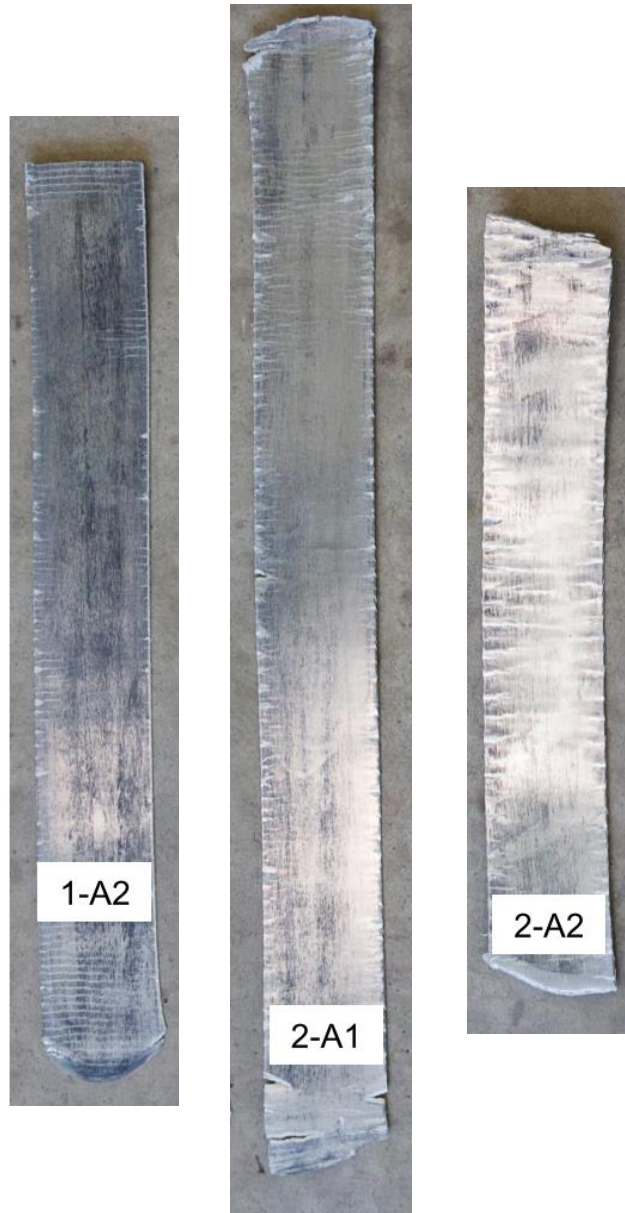


Fig. 44 Macrographs of sheets 1-A2, 2-A1, and 2-A2

Initiating the rolling schedule at a higher furnace temperature of 250 °C resulted in a maximum of 6 passes (plate 3-A1). Lowering the reduction ratios and increasing the temperature to about 275 °C, sheets with a thickness of 2.2 mm were achieved after 10 rolling passes. The best surface quality was reached by rolling at a temperature of about 275 °C and 11 rolling passes (plate 6-A2, see Fig. 45). However, edge cracks with a length of approximately 10 mm were commonly observed on each side of the rolled plates (see Fig. 46). Given the width of the rolled

material, a sheet with a width of about 60 mm without cracks could be fabricated. In turn, these could be used for further investigations. After rolling, the smallest grain size of $2.6 \pm 1.1 \mu\text{m}$ was reached with sheet 5-A1 (see Fig. 46).

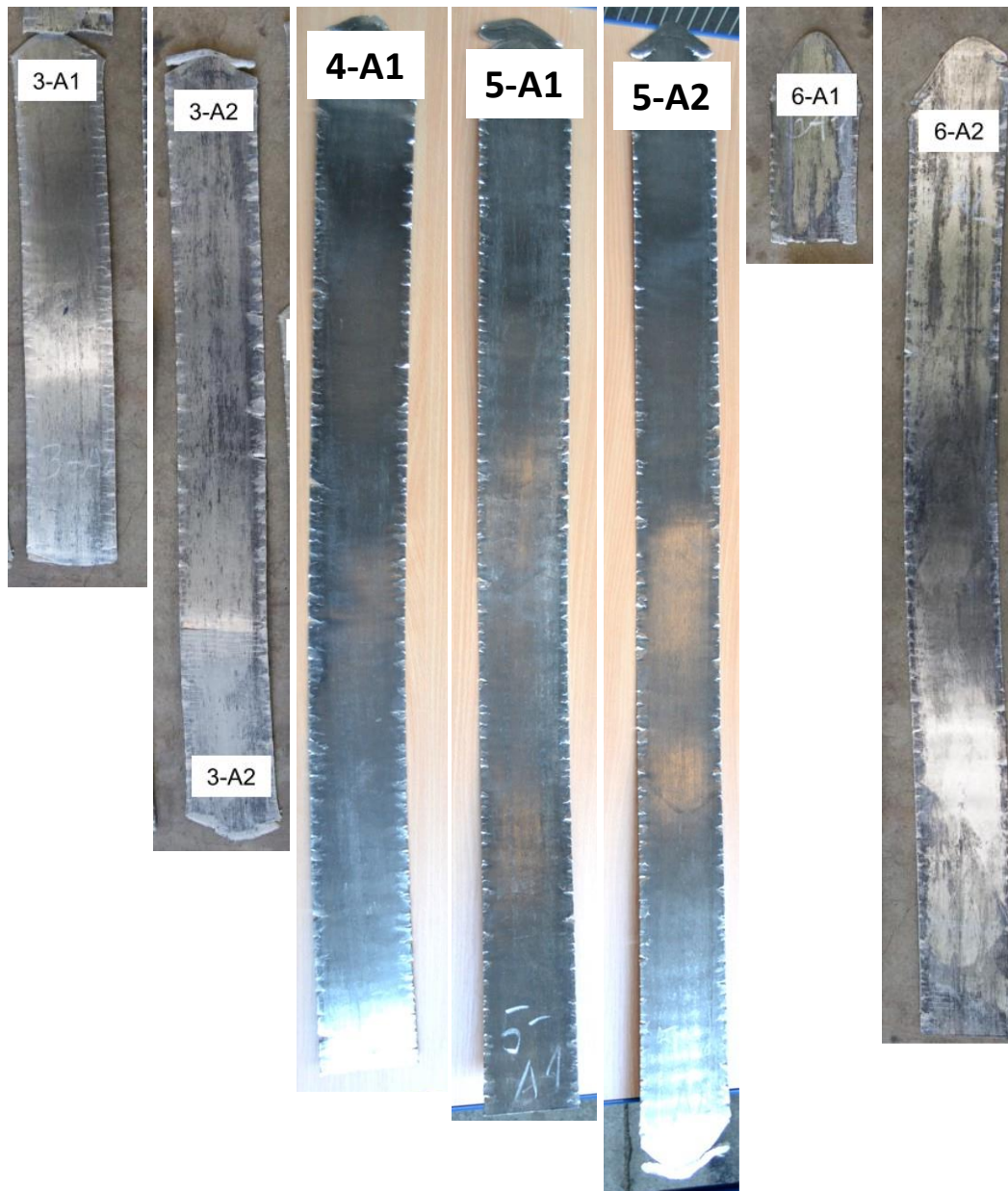


Fig. 45 Macrographs of sheets 3-A1, 3-A2, 4-A1, 5-A1, 5-A2, 6-A1, and 6-A2

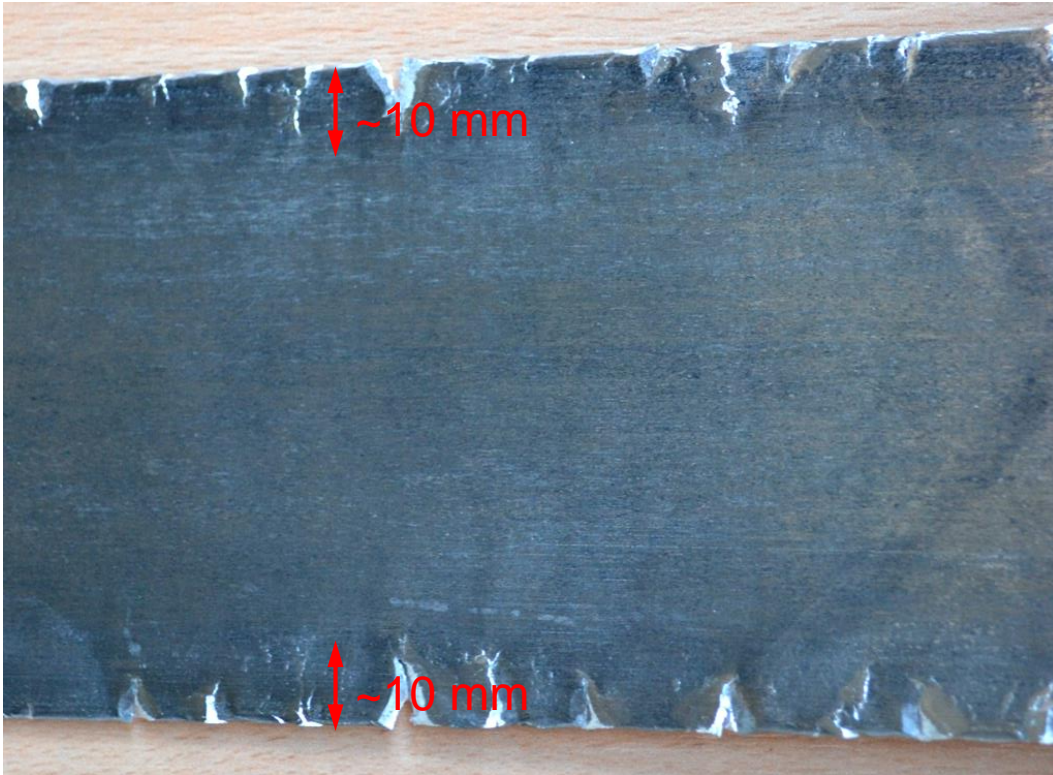


Fig. 46 Edge cracks of sheet 5-A2

In addition to edge cracking, many of the sheets failed by shear. In Fig. 47 a typical example of a failed sheet is shown; the image on the left shows a top view while the image on the right shows the side view of the sheet. Usually, the failed sheets sheared at an angle of about 45° to the rolling direction. The cracks were caused by shear banding due to the low ductility of the material at low rolling temperatures.

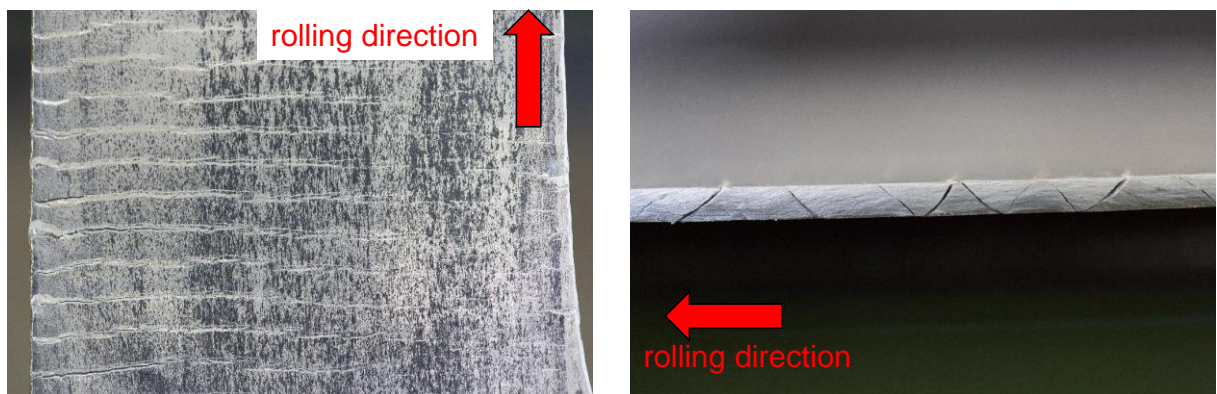


Fig. 47 Shear failure of the rolled sheets

In Figs. 48–50, the results of the microstructural analysis of the as-received approximately 12.5-mm plates from the tooling plate are shown in all 3 directions (x-, y-, and z-; see Fig. 7). The average chord length (or grain size) of the as-received material was determined to be about 25.5 μm in the transverse direction (z-direction). Examination of the 3 sets of figures, at increasing magnification, reveals that this material has an inhomogeneous microstructure. Specifically, regions of smaller grains can be found among regions of much larger grains. This is quite evident in the etched surfaces. Furthermore, a second phase is present as uniformly dispersed particles with a size of about 20–50 μm (see Figs. 48–50).

The rolling procedures were successful in not only reducing the thickness, but also the grain size of the alloy sheet. The measured grain sizes are listed in Table 5. A significant grain size refinement, from about 26 μm in the as-received condition to about 3–4 μm after rolling, was observed for sheets 5-A1 and 6-A2. An accurate measurement of the grain size for sheet 4-A1 after rolling to a thickness of 1.5 mm was not possible because of the prevailing bimodal microstructure. Figure 51 (low magnification images in the upper row) shows that the small second-phase particles are oriented parallel or longitudinal along the rolling direction. At higher magnifications, it can be observed that the original bimodal microstructure of the as-received plate is retained within the sheet 4-A1 (even after 11 passes, at a thickness of 1.5 mm).

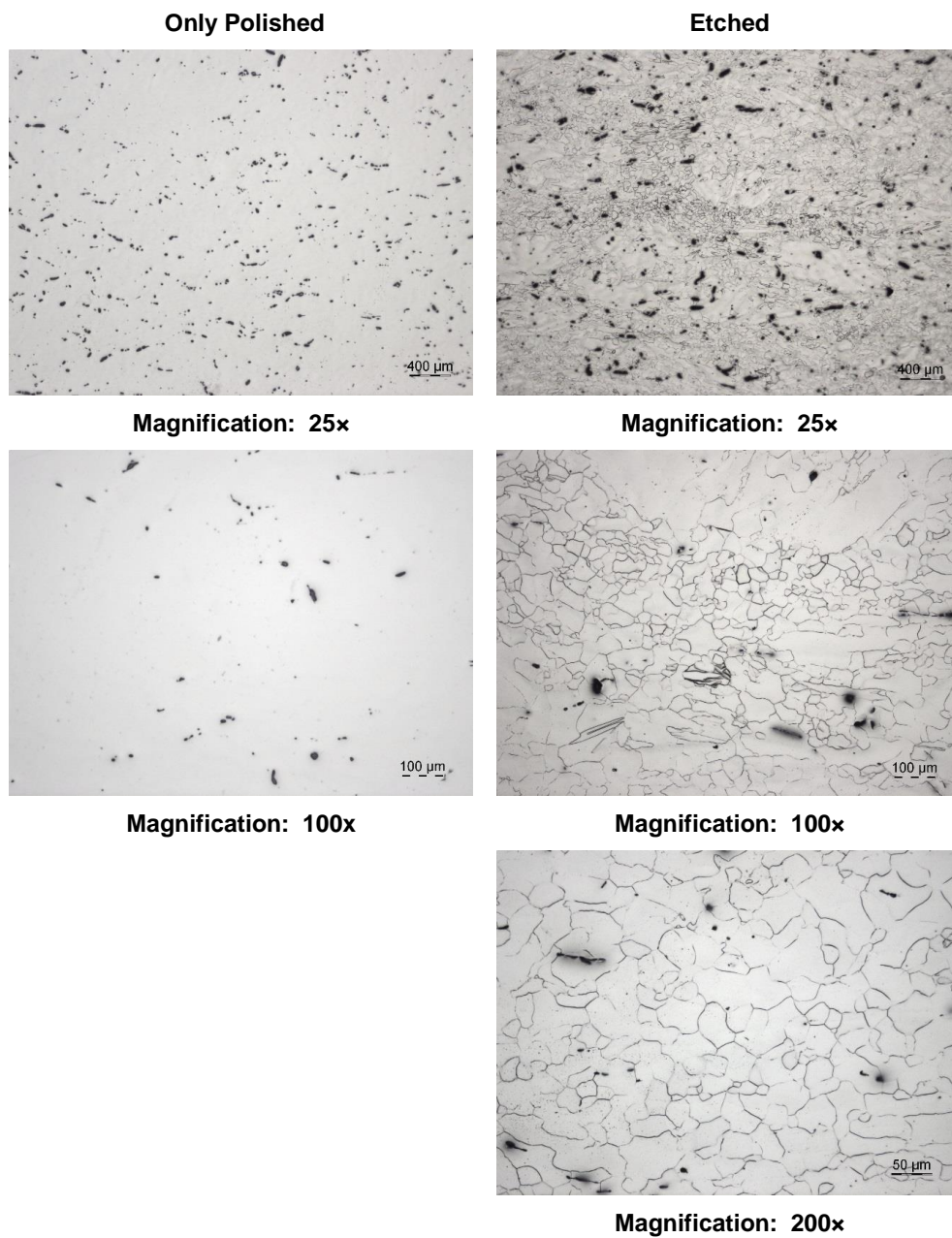


Fig. 48 Microstructure of the as-received material (A-type plates) in the longitudinal direction (x-direction, x-y-plane)

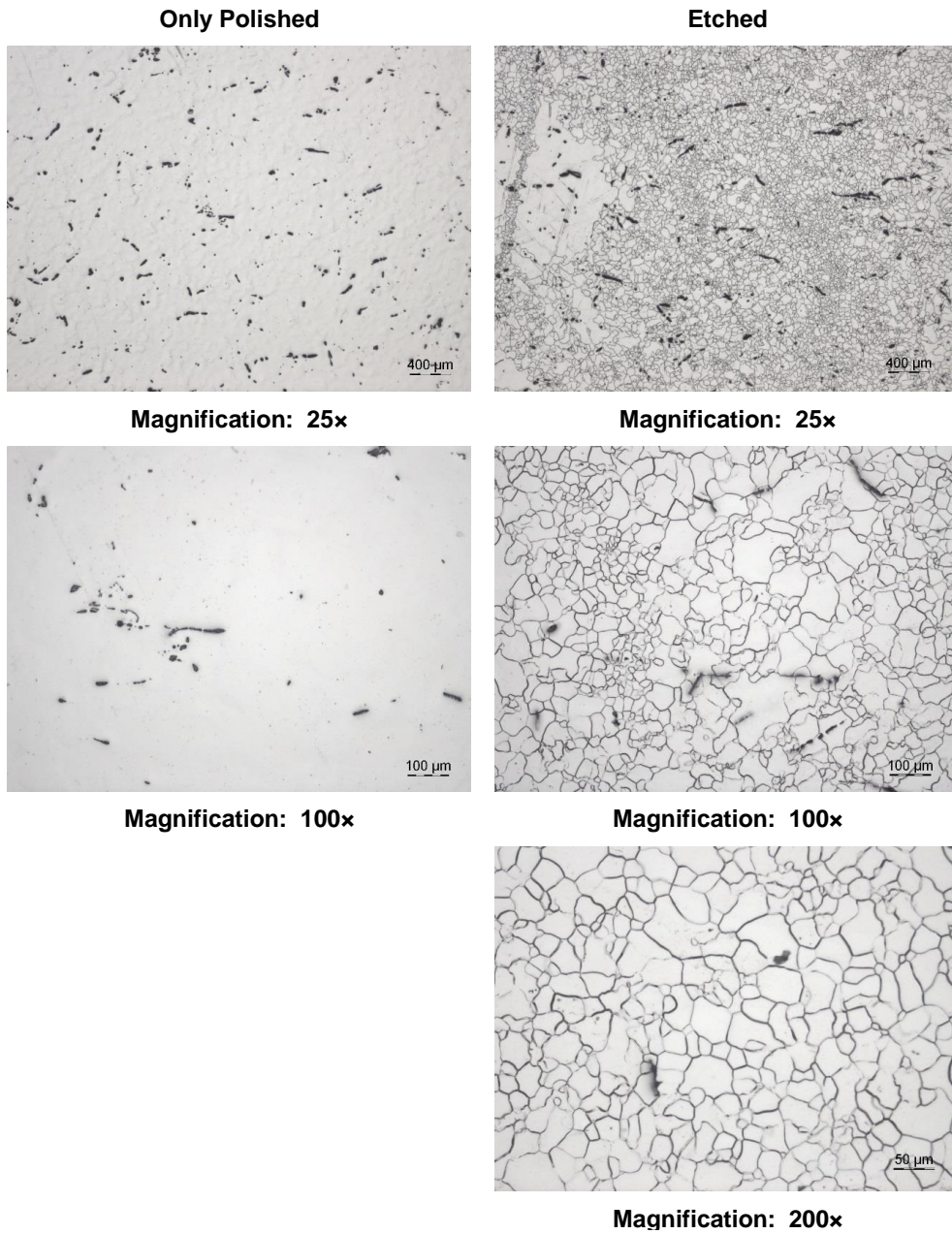


Fig. 49 Microstructure of the as-received material (A-type plates) in the transverse direction (z-direction, y-z-plane)

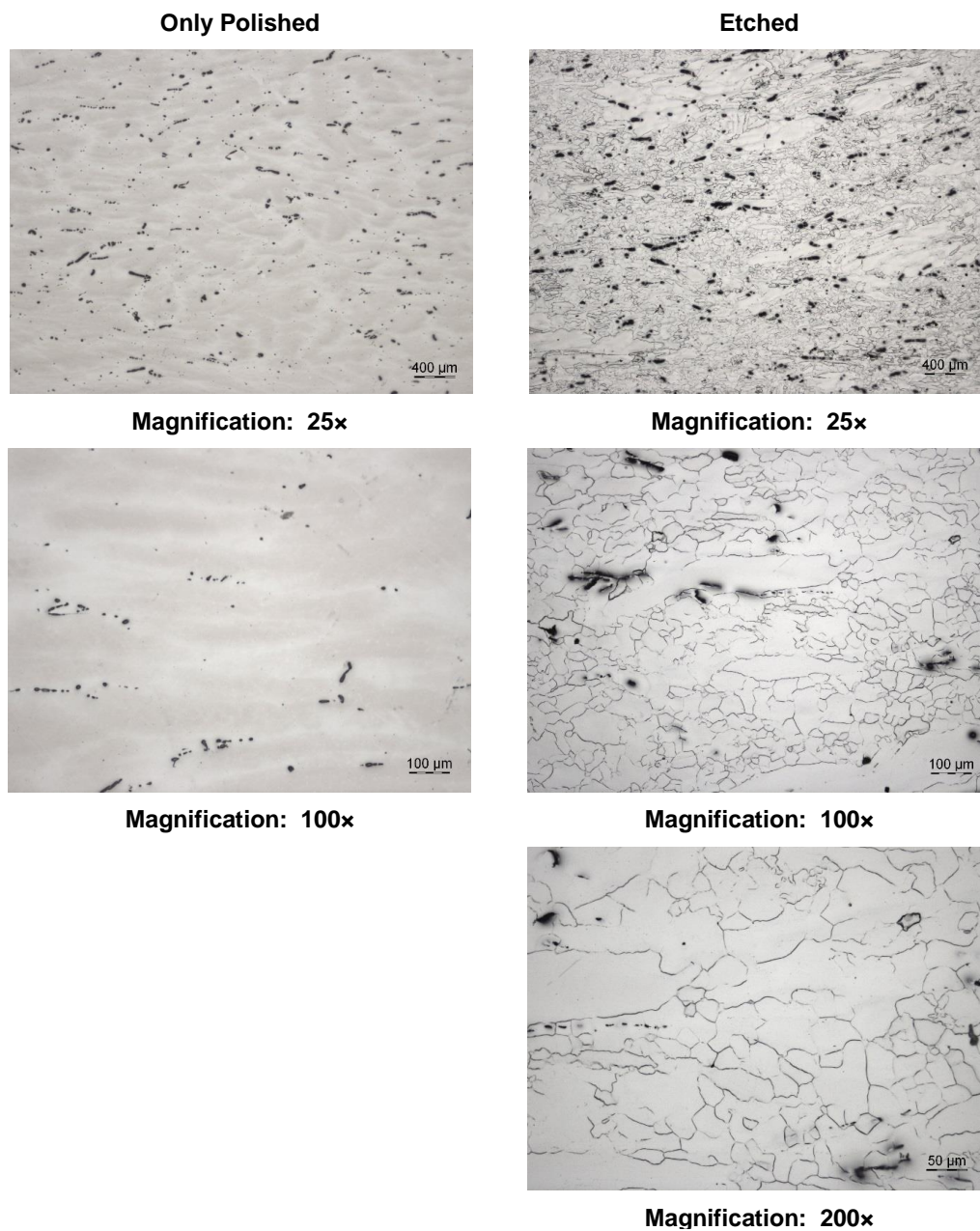


Fig. 50 Microstructure of the as-received material (A-type plates) in the longitudinal direction (y-direction, x-z-plane)

Table 5 Results of rolling passes and average chord length of rolled sheets (longitudinal direction)

Sheet	Thickness (mm)	Number of Rolling Passes	End Temperature after Rolling (°C)	Average Chord (longitudinal) Length (μm)
As-received	~12.5	25.5 ± 11.3 (transverse)
4-A1	3.4	8	209	5.2 ± 1.9
4-A1	1.5	11	227	Not measurable
5-A1	1.5	11	222	2.6 ± 1.1
6-A2	1.5	11	207	4.1 ± 2.0

Only Polished



Magnification: 50×



Magnification: 100×

Etched



Magnification: 200×



Magnification: 500×

Fig. 51 Bimodal microstructure of sheet 4-A1 after rolling to a thickness of 1.5 mm, longitudinal to rolling direction (x-y-plane)

The grain size reduction was also examined for the other sheets. Optical micrographs are oriented longitudinal to the rolling direction for sheet 4-A1 (after 8 passes, thickness 3.4 mm) is shown in Fig. 52. The orientation of the small

particles along the rolling direction can also be clearly observed in these micrographs.

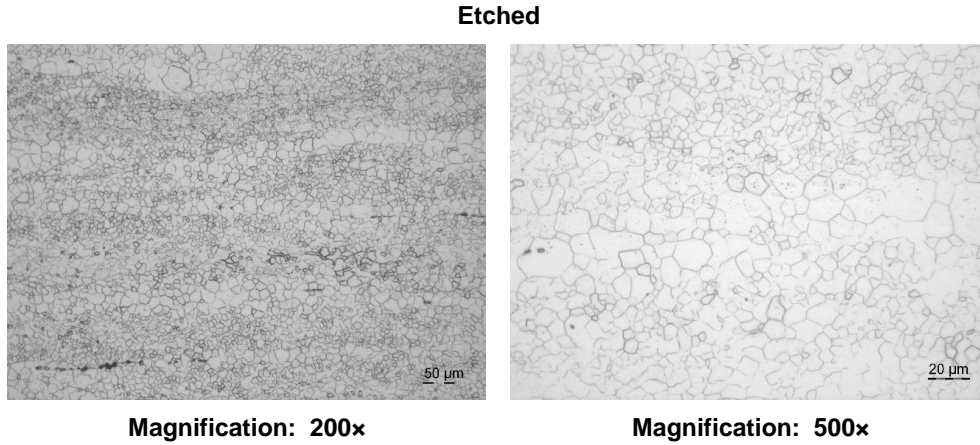


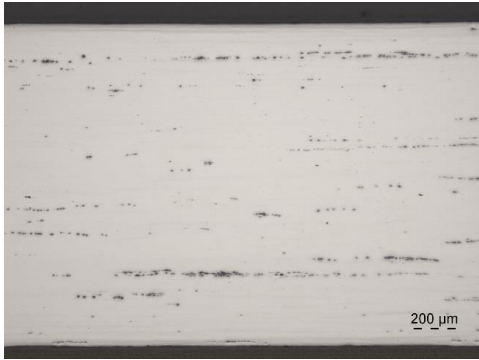
Fig. 52 Microstructure of sheets 4-A1 after rolling to a thickness of 3.4 mm, longitudinal to rolling direction in 2 magnifications (x-y-plane)

Representative images of the microstructure of sheets 5-A1 and 6-A2, respectively, (see Figs. 53 and 54, only polished) are shown, again in the longitudinal orientation, as indicated by the small particles. However, unlike the previous images for sheet 4-A1, the images of the etched microstructure for sheet 5-A1 show a much more homogenous microstructure.

In the transverse direction, the particles are uniformly distributed (see Fig. 55), which could be of advantage under shock loading (spalling). The grain sizes of both sheets 5-A1 and 6-A2 are very fine, about $2.6 \pm 1.1 \mu\text{m}$ and $4.1 \pm 2.0 \mu\text{m}$, respectively. A comparison of the rolling processes of these 2 sheets indicates that larger cracks formed in sheet 5-A1. It is also presumed that there is a higher susceptibility to the occurrence of shear failure for sheet 5-A1.

Based on these observations, it may be concluded that a rolling procedure below 275°C seems to be unreasonable for further rolling experiments. To further summarize, the rolling experiments, the surface condition, resultant microstructure, and the properties of sheet 6-A2 can be considered as the best option for rolling at a decreased temperature. It is proposed that these rolling parameters might be used as the starting point for future investigations on ultrafine-grained plates.

Only Polished



Magnification: 50x



Magnification: 100x

Etched



Magnification: 200x



Magnification: 500x

Fig. 53 Microstructure of sheet 5-A1 after rolling to a thickness of 1.5 mm, longitudinal to rolling direction (x-y-plane)

Only Polished



Magnification: 50×



Magnification: 100×

Etched



Magnification: 200×



Magnification: 500×

Fig. 54 Microstructure of sheet 6-A2 after rolling to a thickness of 1.5 mm, longitudinal to rolling direction (x-y-plane)

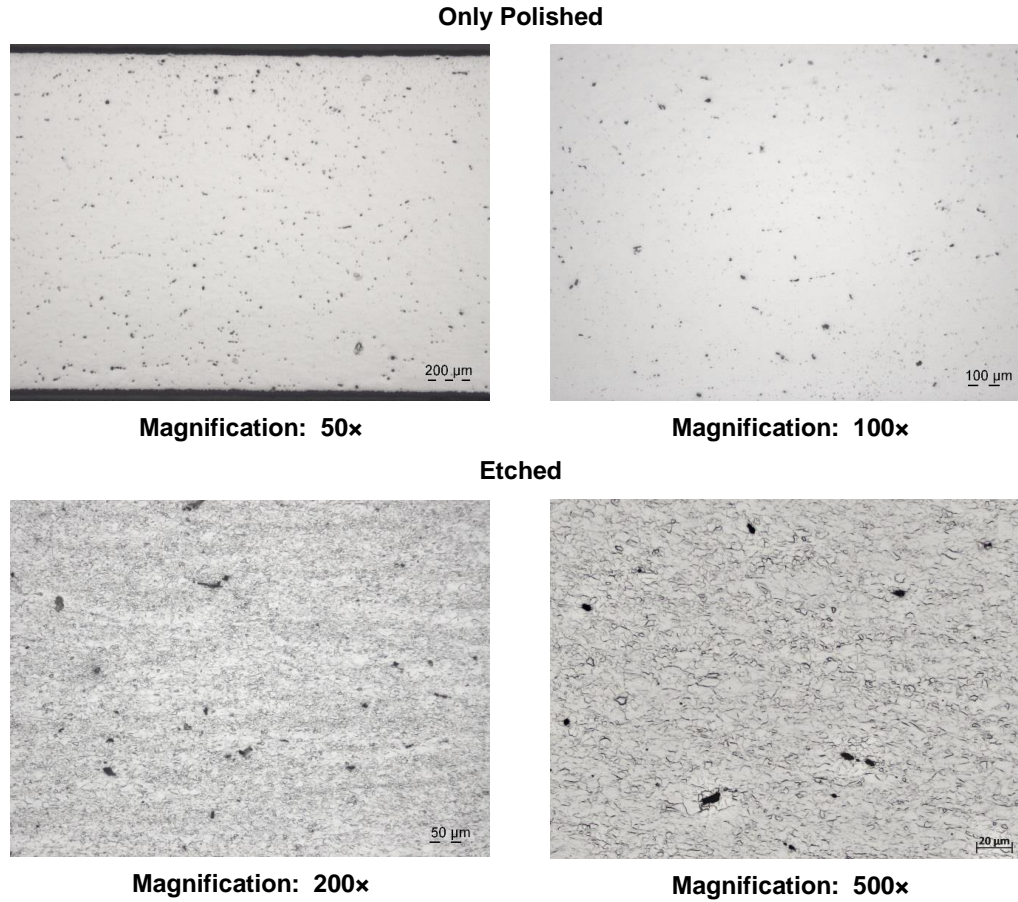


Fig. 55 Microstructure of sheet 6-A2 after rolling to a thickness of 1.5 mm, transverse to rolling direction (x-y-plane)

4.2.2 Rolling Transverse to Original Rolling Direction

In addition to developing the rolling schedule for sheets with A-type plate orientation, sheets with B- and C-type plate orientations were considered in the study. The rolling passes and furnace temperatures for the B- and C-type sheets are listed in Table 6. Recall that the B-type plate has an orientation that is short transverse to the original rolling direction, while the C-type plate is oriented long transverse (see Fig. 7) relative to the original direction. All plates were rolled to a thickness of about 1.3–1.4 mm and a length of about 1.1–1.3 m. However, plates 1-B1, 2-B1, and 2-B2 failed completely by shearing. The rolled sheets are shown in Figs. 56 and 57. A better sheet quality (fewer cracks) can be reached with increased rolling temperature, but this might also cause grain growth and lead to larger grains. As the edge cracks have a length of about 10 mm, the rolled sheets have a width of about 60–70 mm free of cracks.

Table 6 Rolling pass, sheet thickness, and furnace temperature for B- and C-type plates^a

Rolling Pass	Plate Number Sheet Thickness (mm)					
	1-B1	1-B2	2-B1	2-B2	1-C	2-C
1	10.6	10.6	10.6	10.6	10.6	10.6
2	9.0	9.0	8.7	8.8	8.9	8.9
3	6.7	7.3	8.0	8.0	8.0	8.0
4	6.5	6.5	7.2	7.2	7.2	7.2
5	5.8	5.8	6.5	6.5	6.5	6.5
6	5.2	5.2	5.8	5.8	5.8	5.8
7	4.5	4.6	5.2	5.2	5.2	5.2
8	4.2	4.2	4.6	4.5	4.5	4.6
9	3.6	3.6	4.4	4.1	4.1	4.1
10	3.1	3.1	3.6	3.6	3.6	3.6
11	2.8	2.8	3.1	3.1	2.8	2.8
12	2.4	2.4	2.8	2.8	2.2	2.4
13	2.1	2.1	2.4	2.4	1.8	2.1
14	1.8	1.8	2.1	2.1	1.4	1.8
15	1.4	1.4	1.8	1.8		1.4
16			1.4	1.3		
	Failed	Cracks on edge	Failed	Failed	Cracks on edge	Cracks on edge

Furnace temperature (°C) 275

^aIntermediate annealing at 275 °C for 15–30 min

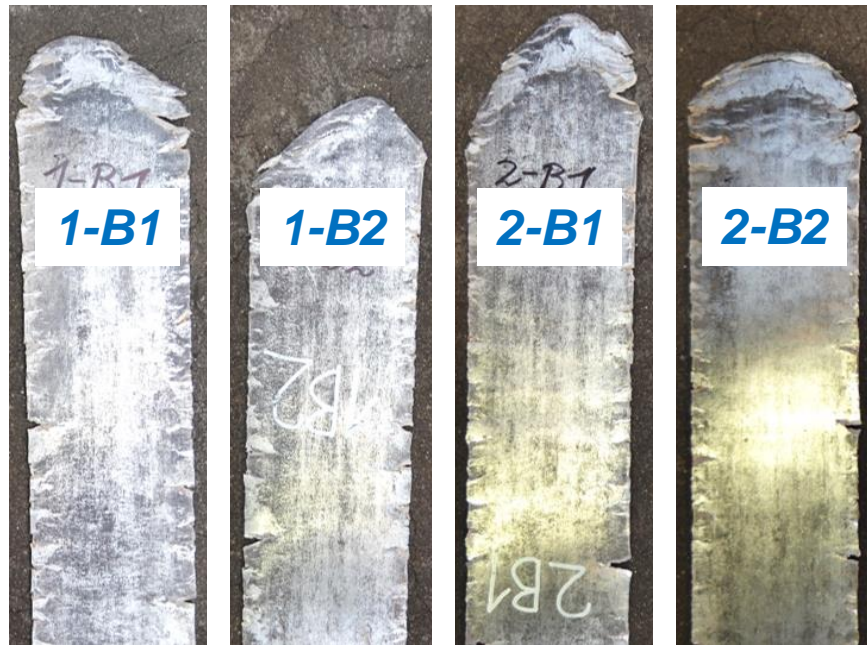


Fig. 56 Rolled B-type sheets 1-B1, 1-B2, 2-B1, and 2-B2

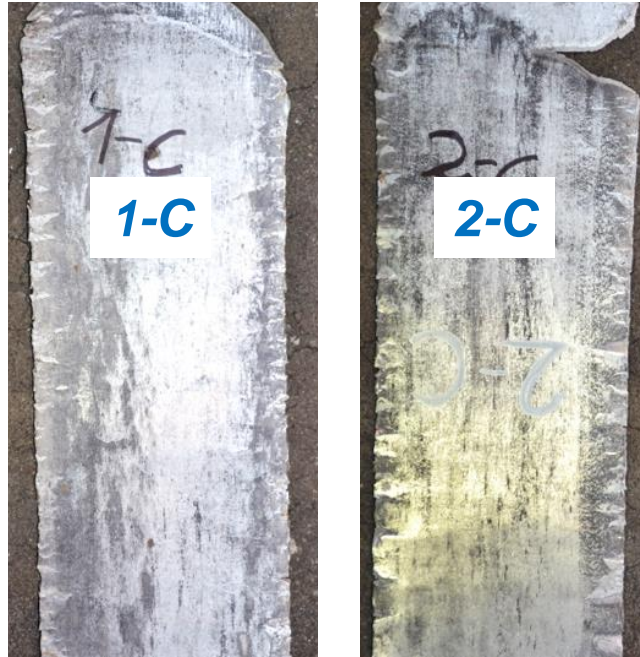


Fig. 57 Rolled C-type sheets 1-C and 2-C

The measured temperatures at the completion of each rolling pass are listed in Table 77. With an increasing number of rolling passes, a decrease of the temperature can be observed. This is due to the decreasing temperature of the rollers, which were preheated before the rolling experiments and were cooling down as the time frame of the experiment increased. At first glance, it might be concluded that the lower temperature in the last few rolling passes may be the cause of edge cracking and failure of the sheets. However, after the second and third rolling pass the first cracks on the sheet edges can already be observed. This is when the temperature of the rolls are nearly at their initial level. Therefore, the cracks that developed cannot be only a result of too low a rolling temperature. Instead, it is supposed that the as-rolled texture of the as-received material might be another reason for the initiation of the cracks.

Table 7 Roller temperature at the completion of each rolling pass for B- and C-type plates^a

Rolling Pass	Plate Number Temperature (°C)					
	1-B1	1-B2	2-B1	2-B2	1-C	2-C
1						
2			255	255	255	255
3	245	245				
4			230	230	230	230
5	215	215				
6			240	240	240	240
7	200	200				
8			220	220	220	220
9	210	210				
10	240	240	220	220	220	220
11			240	240		
12	200	200			200	200
13			200	200		
14	180	180			190	180
15	180	180	170	170		170
16			190	180		
	Failed	Cracks on edge	Failed	Failed	Cracks on edge	Cracks on edge
Furnace temperature (°C)	275					

^aIntermediate annealing at 275 °C for 15–30 min

The results of microstructure investigations after rolling of the B-type sheets to a thickness of about 1.4 mm are shown in Figs. 58 and 59. In the longitudinal and transverse directions, respectively, very fine grains ($\sim 2 \mu\text{m}$) can be found. Furthermore, especially in the transverse direction, there are regions of both fine and coarse grains that can be observed in the higher magnification images. From observation of the polished cross sections, it can be seen that small particles are distributed inhomogeneously and appear as chain-like structures. These particles have a size range of about 10–50 μm .

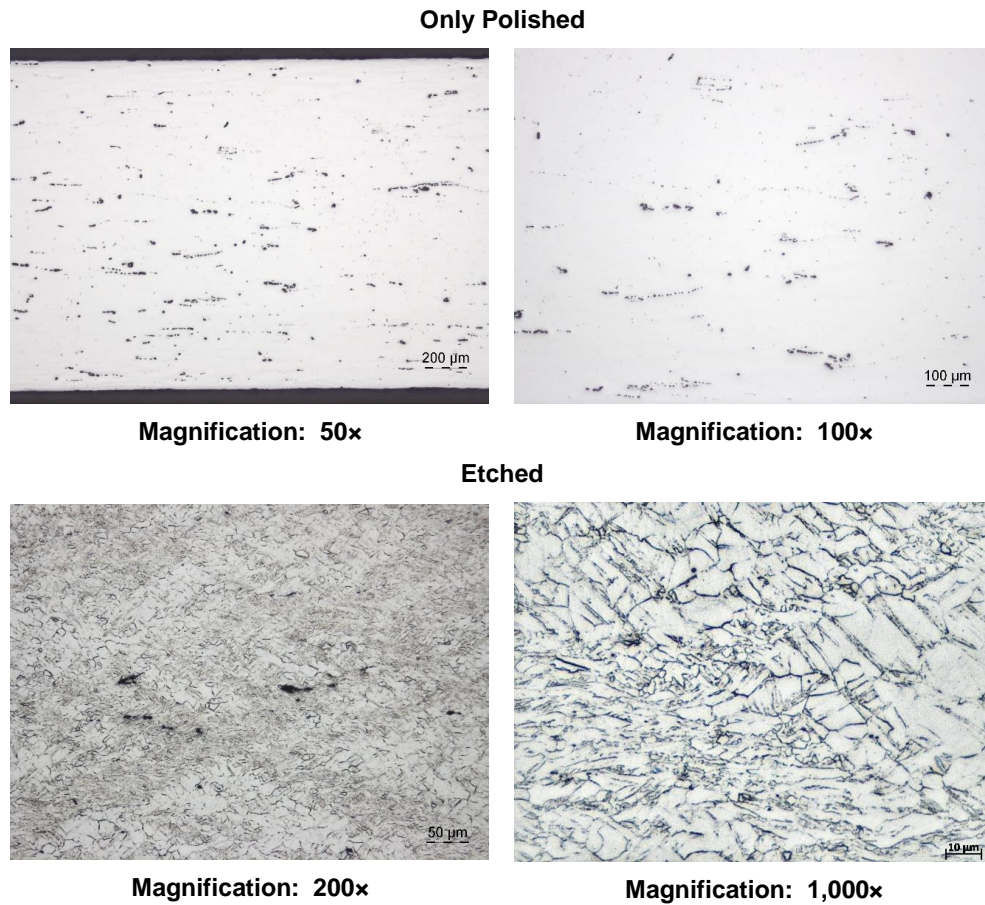


Fig. 58 Microstructure of the 1-B2 sheet after rolling to a thickness of 1.4 mm, longitudinal to rolling direction (x-z-plane)

Only Polished



Magnification: 50x

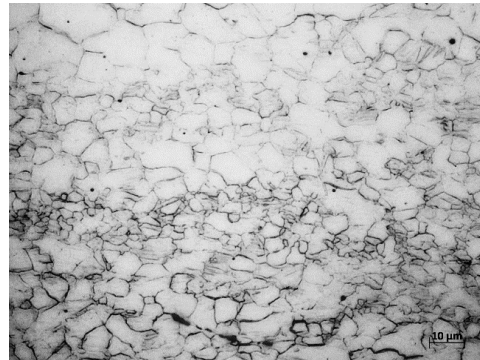


Magnification: 100x

Etched



Magnification: 200x

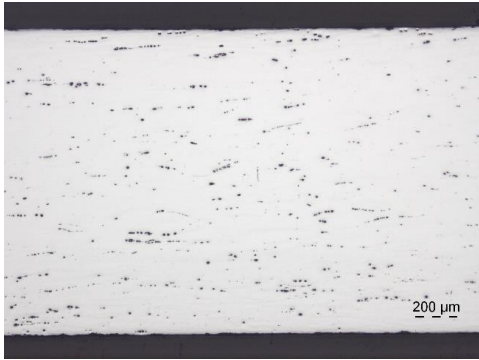


Magnification: 1000x

Fig. 59 Microstructure of the 1-B2 sheet after rolling to a thickness of 1.4 mm, transverse to rolling direction (x-y-plane)

The resulting microstructures after rolling of the C-type sheets to a thickness of about 1.4 mm are shown in Figs. 60 and 61. In both of the longitudinal and transverse directions, a significant bimodal microstructure with fine and coarse grains can be observed. The fine grains have an average size of about 2 μm and the larger grains of about 10–20 μm . The regions of the fine grains are oriented at an angle of about 30° to the rolling direction (y-z plane) (see arrows in Fig. 61). In the transverse direction (x-z plane), these regions of fine grains can be observed as narrow bands (see Fig. 61). It is hypothesized that during rolling, microscale shear bands formed at first then later formed into bands with small grains. Again, the fine particles (only polished micrographs) are oriented in a chain-like manner.

Only Polished

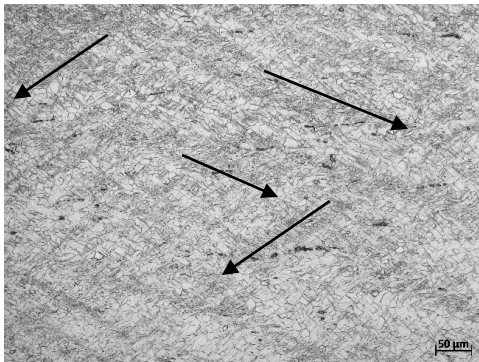


Magnification: 50x

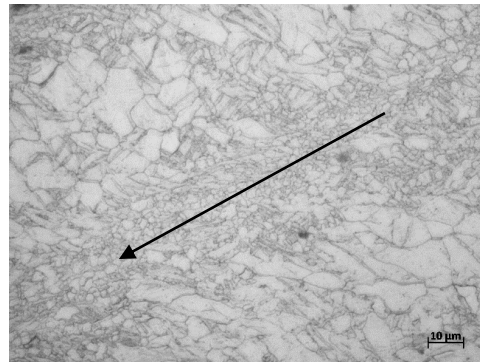


Magnification: 100x

Etched



Magnification: 200x



Magnification: 1,000x

Fig. 60 Microstructure of sheet 2-C after rolling to a thickness of 1.4 mm, transverse to rolling direction (x-z-plane)

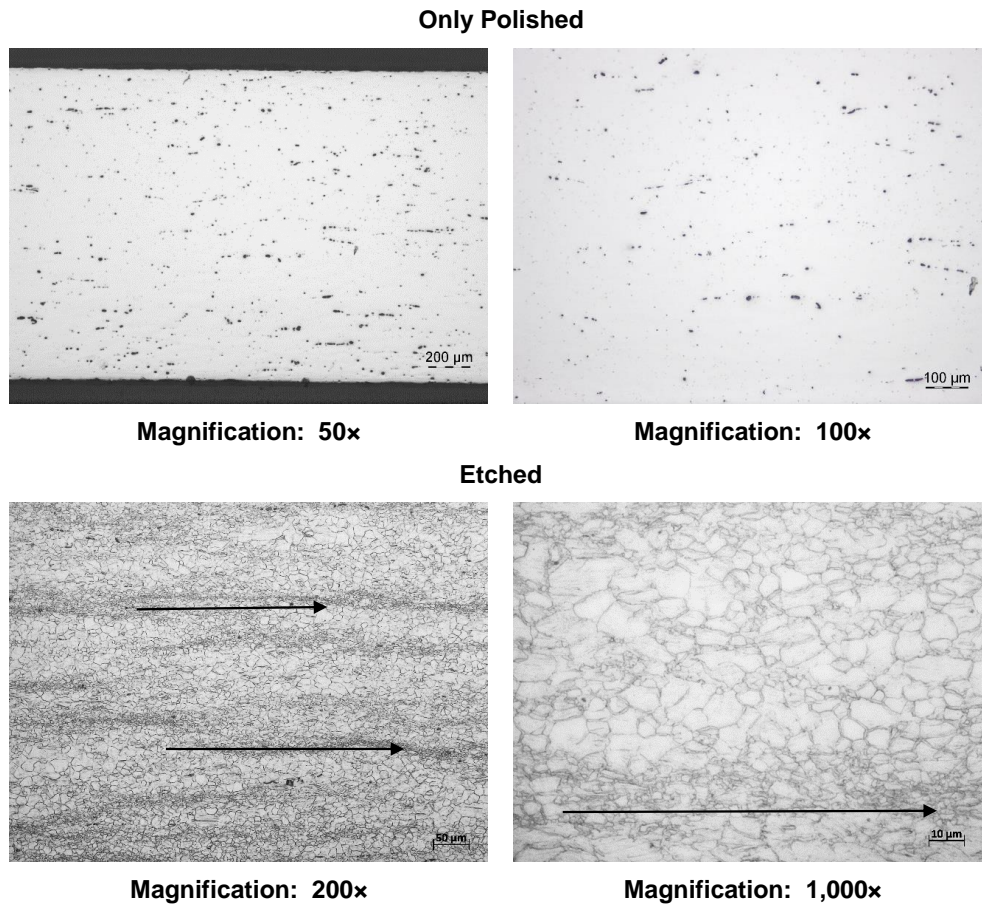


Fig. 61 Microstructure of sheet 2-C after rolling to a thickness of 1.4 mm, transverse to rolling direction (x-z-plane)

The grain sizes of the rolled B- and C-type sheets, 1-B2 and 2-C, are listed in Table 88. Because of the bimodal microstructure, an average grain size was not determined. The grain sizes after final rolling were determined to be 1–13 μm for sheet 1-B2 and 1–12 μm for sheet 2-C. This represents a significant grain refinement compared with 25.5 μm of average grain size (as determined by the chord length method) for the as-received material.

Table 8 Rolling passes, sheet thicknesses in millimeter and average chord length of rolled sheets B and C (transverse direction)

Plate	Thickness (mm)	Number of Rolling Passes	Grain size (transverse) (μm)
As-received	~12.5	...	25.5 ± 11.3 (average chord length)
1-B2	1.4	15	1.3–13.3
2-C	1.4	15	0.8–11.9

5. Summary

The results of the rolling experiments with an initially “coarse” grain structure are very promising. With temperatures of about 275 °C, it has been shown that Mg sheets about 1.3–1.5 mm thick could be produced. The rolling process may further be optimized with an as-received material, which is characterized by the following:

- Good ductility in the parallel (longitudinal) direction to the rolling direction (A-type plates).
- A uniform and homogeneous microstructure with a grain size below 20 μm .
- High surface finish quality with few, if any, surface cracks.
- Few impurities that are more homogeneously distributed in the bulk.

For further rolling experiments, a rolling temperature of at least 275 °C coupled with no more than a 10% thickness reduction per rolling pass is recommended. Furthermore, an intermediate annealing treatment should be used after the third rolling pass.

This investigation into developing a rolling procedure should be repeated with a finer-grained material, specifically obtained possibly through ECAE. It is hypothesized that the finer microstructure of the ECAE material, using a rolling direction that is parallel to the extrusion direction imposed by the ECAE process, will lead to an improvement in rolling results. With a rolling temperature of about 275 °C and a demonstrated grain refinement, as the microstructural investigation presented in this report showed, it is expected that no grain growth of the ECAE material should occur.

6. Conclusions

The first series of rolling experiments with plates 12.5 mm thick was performed at a constant temperature of 425 °C, following a prehomogenization treatment at about 440 °C for 1 h. Using this approach, sheets about 1.5 mm thick were produced without obvious cracks and had very good surface qualities. A significant grain refinement resulted from this rolling process, reducing in grain size from about 20–50 µm for the as-received material down to about 5–8 µm after 7–8 rolling passes. After rolling, tensile tests determined that the difference between 2 parallel specimens taken from the same orientation is very low. In addition, a 1% higher yield strength ($\sigma_{1\%}$ ~210–245 MPa) and a UTS of approximately 280 MPa were observed for the as-rolled material compared with the as-rolled and annealed material. The elongations to failure (~18%–23%) were nearly the same for all of the samples. The little variation between samples indicated that a final annealing treatment at 330 °C, and 0.5 h was not necessary.

The second series investigations of rolling the material with decreasing the rolling temperature demonstrated that the as-received material can be rolled at temperatures as low as about 275 °C (furnace temperature). This procedure resulted in inducing small cracks on the edges of the sheets. These edge cracks have a depth or length of about 10 mm. However, the sheets have a useable width of about 60–70 mm between the cracks, and thus can be used for further investigations.

Microscopic examination of this alloy revealed considerable grain size reduction in both series of rolling trials. The as-received material is characterized by a bimodal microstructure with smaller fine (~15 µm) and much larger coarse grains (up to 100 µm). With rolling temperatures of about 275 °C, the as-received average grain size of about 25.5 µm was reduced to a grain size of 2–4 µm for sheets with A-type orientation and about 1–13 µm for sheets with B- and C-type orientations after rolling to about 1.3–1.5 mm. After final rolling, a significant bimodal microstructure with small grains of about 2–3 µm and larger grains about 10–20 µm was observed.

This means that the as-received microstructure was refined by a factor of 10–20. Furthermore, oriented chain-like particles of sizes between 10–50 µm were observed in the as-received material. The nonuniformity of the material caused by these particles and the initial bimodal microstructure are believed to be the main reasons for the initiation of cracks immediately after the first rolling passes. Smaller grains and a more homogeneous microstructure is expected with a more homogeneous and fine-grained as-received microstructure, as well as with a better dispersion of

impurities and intermetallic precipitate particles. Similarly, better surface finish and quality should result if a thinner starting material with an as-received thickness of about 6 mm is used. This will also lead to a lower degree of deformation per pass using a fewer number of passes, resulting in better grain refinement.

7. References

1. Hammond VH, Mathaudhu SN, Doherty KJ, Walsh SM, Vargas LR, Placzankis BE, Labukas JP, Pepi MS, Trexler MD, Barnett BD, Jones TL, Kecskes LJ. Ultrahigh-strength magnesium alloys for the future force: a final report on the 5-year mission program, 2009–2013. US: Aberdeen Proving Ground (MD): Army Research Laboratory (US); 2014. Report No.: ARL-TR-6788. Also available at: <http://www.arl.army.mil/arlreports/2014/ARL-TR-6788.pdf>.

List of Symbols, Abbreviations, and Acronyms

Al	aluminum
ARL	US Army Research Laboratory
ECAE	equal channel angular extrusion
Mg	magnesium
ORD	original rolling direction
UTS	ultimate tensile strength

1 DEFENSE TECHNICAL
(PDF) INFORMATION CTR
DTIC OCA

2 DIRECTOR
(PDF) US ARMY RESEARCH LAB
RDRL CIO LL
IMAL HRA MAIL & RECORDS
MGMT

1 GOVT PRINTG OFC
(PDF) A MALHOTRA

12 DIR USARL
(PDF) RDRL WMM
J BEATTY
R DOWDING
J ZABINSKI
RDRL WMM F
K DARLING
V HAMMOND
L KECSKES
E Klier
H MAUPIN
T SANO
M TSCHOPP
RDRL WMM D
R CARTER
S WALSH